

GNBG: A Generalized and Configurable Benchmark Generator for Continuous Numerical Optimization

Danial Yazdani*, Mohammad Nabi Omidvar*, Delaram Yazdani, Kalyanmoy Deb, and Amir H. Gandomi†

Abstract

As optimization challenges continue to evolve, so too must our tools and understanding. To effectively assess, validate, and compare optimization algorithms, it is crucial to use a benchmark test suite that encompasses a diverse range of problem instances with various characteristics. Traditional benchmark suites often consist of numerous fixed test functions, making it challenging to align these with specific research objectives, such as the systematic evaluation of algorithms under controllable conditions. This paper introduces the Generalized Numerical Benchmark Generator (GNBG) for single-objective, box-constrained, continuous numerical optimization. Unlike existing approaches that rely on multiple baseline functions and transformations, GNBG utilizes a single, parametric, and configurable baseline function. This design allows for control over various problem characteristics. Researchers using GNBG can generate instances that cover a broad array of morphological features, from unimodal to highly multimodal functions, various local optima patterns, and symmetric to highly asymmetric structures. The generated problems can also vary in separability, variable interaction structures, dimensionality, conditioning, and basin shapes. These customizable features enable the systematic evaluation and comparison of optimization algorithms, allowing researchers to probe their strengths and weaknesses under diverse and controllable conditions.

Index Terms

Global optimization, Benchmark generator, Test suite, Performance evaluation, Optimization algorithms.

I. INTRODUCTION

Optimization algorithms have been the subject of intense research and development over the past decades, with applications spanning a variety of domains, such as data science [1], engineering [2], and transportation [3]. Despite these advancements, a pressing challenge remains: the reliable and comprehensive benchmarking of these algorithms. A fundamental research question in this context is to ascertain how effectively an algorithm performs on problems that present specific characteristics, challenges, and levels of difficulty. While theoretical analyses offer insights, they can be prohibitively difficult to conduct for complex algorithms and intricate problem instances. Consequently, empirical evaluation becomes the method of choice, typically executed by solving a predefined set of benchmark problem instances [4].

To ensure the robust design and efficacy of optimization algorithms, the use of standardized benchmark test suites is essential [5]. These suites often consist of mathematical functions with known characteristics, thereby enabling researchers to investigate the strengths and weaknesses of various optimization methods under different conditions [6]. Utilizing benchmarks with known properties facilitates the study of algorithmic behavior during the optimization process. By offering a standardized basis for comparison, benchmark test suites not only facilitate the development of more effective optimization algorithms but also propel the field of optimization forward.

A proper benchmark test suite should be designed to be easy to understand and facilitate a clear understanding of optimization algorithms and their behavior within the search space. This aids researchers in visualizing the intended search behavior and identifying the weaknesses and strengths of the optimization algorithms. By analyzing the performance of algorithms in this manner, researchers can systematically modify the algorithms, ultimately leading to improved performance. The following are several key characteristics that are generally considered important for a comprehensive benchmark suite [7, 8].

Danial Yazdani is with the Faculty of Engineering & Information Technology, University of Technology Sydney, Ultimo 2007, Australia. (e-mail: danial.yazdani@gmail.com)

Mohammad Nabi Omidvar is with the School of Computing, University of Leeds, and Leeds University Business School, Leeds LS2 9JT, United Kingdom. (e-mail: m.n.omidvar@leeds.ac.uk)

Delaram Yazdani is with the Liverpool Logistics, Offshore and Marine (LOOM) Research Institute, Faculty of Engineering and Technology, School of Engineering, Liverpool John Moores University, Liverpool L3 3AF, United Kingdom. (e-mail: delaram.yazdani@yahoo.com)

Kalyanmoy Deb is with the BEACON Center, Michigan State University, East Lansing, MI, 48824, USA. (e-mail: kdeb@egr.msu.edu)

Amir H. Gandomi is with the Faculty of Engineering & Information Technology, University of Technology Sydney, Ultimo 2007, Australia. He is also with the University Research and Innovation Center (EKIK), Obuda University, Budapest 1034, Hungary. (e-mail: Gandomi@uts.edu.au)

*Danial Yazdani and Mohammad Nabi Omidvar contributed equally to this work.

†Corresponding author: Amir H. Gandomi

Diversity: An ideal benchmark test suite should encompass a diverse collection of problem instances that exhibit a range of problem characteristics encountered in practical applications [9–11]. This diversity enables a comprehensive evaluation and comparison of optimization algorithm performance under various conditions. In addition, the inclusion of different major characteristics across problem instances allows researchers to investigate the individual impact of each problem characteristic on the behavior of optimization algorithms.

Complexity Variety: A proper benchmark test suite should encompass problem instances that span a range of complexity levels [12], determined by various factors such as modality (unimodal to highly multimodal), dimensionality, separability, conditioning, and deceptiveness [13]. This enables researchers to thoroughly examine the performance of optimization algorithms across problem instances with different levels of difficulty.

Algorithmic Neutrality: To ensure a fair evaluation of optimization algorithms, a benchmark test suite should mitigate certain problem characteristics that inherently favor specific algorithms/operators. For example, symmetric problem instances, which are in favor of algorithms that rely on Gaussian distributions for generating new solutions [6], problem instances with the optimum positioned on the boundary, which can advantage methods utilizing absorption boundary handling [14, 15], and problem instances with the optimum located at the center of the search space, favoring certain population initialization methods [16], should be avoided [4].

Representativity: The ultimate goal of any benchmarking exercise is to draw robust conclusions about the performance of algorithms. To make these conclusions as accurate and generalizable as possible, the benchmark suite should closely mirror the characteristics, complexities, and challenges commonly encountered in real-world problems [17]. This representativeness ensures that the performance claims made at the end of a benchmarking exercise are both robust and meaningful. The problem instances included in the benchmark suite should thus be carefully chosen to encapsulate the range of difficulties and characteristics typical of real-world scenarios [12].

Configurability: Configurability is a critical aspect of a benchmark suite, providing researchers with the ability to make fine-grained adjustments to a wide range of problem characteristics. This includes, but is not limited to, dimensionality, conditioning, complexity of variable interaction structures, and other morphological features of the problem instances. It is worth noting that the ability to configure the number of dimensions is often referred to as scalability [6, 18]. This aspect of configurability ensures that the benchmark suite can accurately represent the varying scales of real-world problems, thereby enabling a more comprehensive and inclusive evaluation. Overall, the configurability of a benchmark suite offers researchers the flexibility to tailor problem instances to align with specific research objectives or to mimic particular real-world conditions.

Known characteristics and optimal solution(s): The benchmark test suite should provide information on the morphological characteristics, the major challenges, and the position and value of the optimal solution(s) for each problem instance [19]. This information plays a vital role in analyzing the convergence behavior, performance, strengths, and weaknesses of optimization algorithms.

Accessibility: A comprehensive benchmark test suite should include publicly available source code and documentation, ensuring accessibility to the research community.

Numerous benchmark suites exist in the literature to evaluate and compare the performance of optimization algorithms across different sub-fields, such as large-scale optimization [18], multi-objective optimization [20], dynamic optimization [21], and constrained optimization [22]. However, the focus of this paper is specifically on the realm of box-constrained continuous single-objective global optimization, a sub-field that seeks to identify the global optimum of a given optimization problem within a specified search range.

Benchmarking in this context involves comparing the optimal solutions obtained by different algorithms using a range of performance indicators [23]. Such global optimization problems are pervasive in various fields, particularly in mathematics and engineering disciplines [24]. Employing appropriate benchmark test suites in this domain is not just an academic exercise; it lays the foundation for advancements in more complex optimization problems, including dynamic [25, 26], constrained [27], large-scale [28, 29], niching [30], and multi-objective optimization [31]. Therefore, the contributions in this area have broad ramifications that extend across multiple domains of optimization [32]. For the sake of brevity, the term ‘optimization’ used throughout the rest of this paper should be understood to refer specifically to ‘box-constrained continuous single-objective global optimization.’

Traditionally, most benchmarking approaches have relied on a collection of well-established mathematical functions, such as the Sphere, Ellipsoid, Rosenbrock, Rastrigin, Schwefel, Griewangk, and Ackley functions [33–37]. Often, these functions are subjected to standard transformations such as translation (shift) and rotation to simulate a wider range of problem characteristics [6, 38, 39]. However, this approach has the following limitations.

- Firstly, the inherent characteristics of these mathematical functions are generally predefined and fixed, which limits flexibility for fine-grained analysis. While these suites aim for comprehensive coverage by incorporating a wide array of mathematical functions, this abundance can actually complicate the task of effectively navigating and understanding the benchmark suite. As a result, analyses may not adequately reveal the strengths and weaknesses of algorithms across diverse problem characteristics.

- Secondly, existing benchmark suites often lack the ability to configure and control specific problem characteristics, thereby hampering targeted evaluations. This limitation can be a significant obstacle for researchers aiming to delve deeper into how optimization algorithms handle specific problem characteristics under various configurations, such as different degrees of conditioning and complexity of variable interaction structure.

In light of these limitations, this paper introduces the Generalized Numerical Benchmark Generator (GNBG), a configurable, flexible, and user-friendly tool explicitly designed to embody the desirable properties of an effective benchmark suite. Unlike conventional benchmark suites that rely on a variety of fixed mathematical functions, GNBG employs a single, parametric baseline function capable of generating a diverse range of problem instances with controllable characteristics and levels of difficulty. By manipulating various parameters within GNBG, users gain the ability to tailor the properties of the generated problem instances, including:

- **Modality:** GNBG offers the versatility of generating a diverse range of problem instances, from those that feature smooth, unimodal search spaces to instances characterized by highly multimodal and rugged landscapes. This adaptability allows researchers to assess how well optimization algorithms navigate different types of terrain, thereby providing a more comprehensive evaluation of their capabilities.
- **Local Optima Characteristics:** GNBG constructs its search space through the integration of multiple independent components, each having its own ‘basin of attraction’—essentially, a zone where solutions tend to converge. Users can configure various aspects of these components, such as their locations, optimum values, and morphological features. This high level of control extends to the characteristics of any local optima within these basins, allowing for customization of their number, size, width, depth, and shape.
- **Gradient Characteristics:** GNBG allows users to control not just the steepness of the components but also the specific rate of change or curvature of their basins. Users have the flexibility to define these characteristics on a per-component basis, with options ranging from highly sub-linear to super-linear rates of change.
- **Variable Interaction Structures:** GNBG offers a nuanced control over the interactions between variables within generated problem instances. Users can then apply customization rotation matrices to configure variable interactions, allowing for a wide range of interaction structures from fully separable to fully-connected non-separable. GNBG allows users to set the strength of these interactions, ensuring a more robust evaluation of algorithms. Additionally, different regions of the search space can have distinct variable interaction structures, as each component possesses its own localized variable interaction pattern.
- **Conditioning:** GNBG provides users with the ability to generate components with a wide range of condition numbers, spanning from well-conditioned to severely ill-conditioned components. By independently stretching each component along each dimension, users have control over the condition number, allowing them to simulate the challenges posed by ill-conditioning.
- **Symmetry:** GNBG affords the flexibility to generate both symmetric and highly asymmetric problem instances. This is achieved by allowing the strategic distribution of components with varied morphological characteristics across the search space, thereby influencing the symmetry of the resulting problem instances. Furthermore, GNBG provides the capability to generate components with asymmetric basins of attraction. The ability to introduce asymmetry serves an important role in unbiased evaluations; symmetric search spaces can potentially favor algorithms that rely on Gaussian distribution-based operators [6]. Therefore, incorporating asymmetric elements allows for more impartial assessments of algorithmic performance.
- **Deceptiveness:** GNBG affords users the flexibility to introduce various degrees of deception into problem instances. By manipulating the size, location, and depth of components, one can engineer situations that present specific challenges for optimization algorithms. Scenarios can be constructed where, for instance, the global optimum is a narrow peak obscured within the basin of a wider local optimum, or where there is substantial separation between high-quality local optima and the global optimum. This enables researchers to scrutinize how well algorithms can navigate misleading or complex landscapes, thereby yielding insights into their robustness and efficacy.
- **Scalability:** All problem instances generated by GNBG are scalable with respect to dimensionality.

While the user has insights into the characteristics of problem instances generated by GNBG, it is crucial to note that these instances are treated as black boxes by the optimization algorithms. That is, the algorithms operate without access to the internal structure or specific properties of these instances, interacting solely through the evaluation of candidate solutions and the function values they receive. This approach ensures an authentic assessment of an algorithm’s ability to effectively navigate and explore a problem space, uninformed by any prior knowledge of specific problem characteristics.

The utility of a configurable benchmark generator like GNBG lies in its ability to create problem instances with adjustable features, granting researchers an opportunity for nuanced evaluation. Researchers can systematically investigate an algorithm’s strengths and weaknesses under a variety of controlled conditions, a process indispensable for the algorithm’s development and refinement. In turn, GNBG stands to make a significant contribution to the advancement of the field of global optimization by facilitating the creation and analysis of increasingly efficient and effective optimization algorithms.

The main contributions of GNBG can be summarized as follows:

- GNBG operates on a foundational, generalized framework using a singular parametric baseline function.
- GNBG offers the flexibility to generate a multitude of problem instances, each presenting controllable degrees of challenges and various characteristics, allowing researchers to tailor them to specific research objectives.
- One of GNBG's hallmark features is its ability for isolated challenge evaluation. It can uniquely craft problem instances that spotlight specific challenging characteristics at varying intensities.
- GNBG meets all the requisites of an exemplary benchmark, encompassing attributes such as diversity, varied complexity, algorithmic neutrality, representativity, configurability, scalability, known characteristics and optimal solutions, and accessibility.

The rest of this paper is organized as follows. Section II delves into the details of GNBG, explaining its architecture and shedding light on how different parameter settings impact problem characteristics. Section III outlines how GNBG can be used to generate problem instances with specific characteristics. Section IV presents a preliminary empirical study that explores the influence of various problem characteristics on the performance of a selection of optimization algorithms. Finally, Section V concludes the paper, summarizing key findings and implications.

II. GENERALIZED NUMERICAL BENCHMARK GENERATOR

In this section, we provide a comprehensive exposition of the Generalized Numerical Benchmark Generator (GNBG). We commence with the presentation of the baseline mathematical function that acts as the nucleus of GNBG, around which the test instances are constructed. Subsequently, we delve into the parameters of GNBG and scrutinize their roles in shaping the attributes of the optimization challenges generated¹.

A. Baseline Mathematical Formulation

The search space in GNBG is a composite landscape formed by aggregating multiple distinct components, each characterized by its unique basin of attraction. These components, which must all have the same dimensionality, contribute individual challenges and complexities to the overall search space.

To elucidate how these components and their attributes translate into a comprehensive optimization problem, we now introduce the baseline function of GNBG. The function is expressed as:

$$\begin{aligned} \text{Minimize } : f(\mathbf{x}) &= \min_{k \in \{1, \dots, o\}} \left\{ \sigma_k + \left(\mathbb{T}_k \left((\mathbf{R}_k(\mathbf{x} - \mathbf{m}_k))^{\top} \right) \mathbf{H}_k \mathbb{T}_k \left(\mathbf{R}_k(\mathbf{x} - \mathbf{m}_k) \right) \right)^{\lambda_k} \right\}, \\ \text{Subject to } : \mathbf{x} \in \mathbb{X} : \mathbb{X} &= \{\mathbf{x} \mid l_i \leq x_i \leq u_i\}, i \in \{1, 2, \dots, d\}, \end{aligned} \quad (1)$$

where $f(\cdot)$ represents the GNBG function aimed to be minimized. Here, d indicates the number of dimensions, and \mathbb{X} denotes the d -dimensional search space where \mathbf{x} is a candidate solution. The search space is confined within the bounds l_i and u_i for each dimension i . The term o enumerates the number of components, each contributing to the complexity of the problem with its own set of parameters such as σ_k , \mathbf{m}_k , \mathbf{H}_k , \mathbf{R}_k , and λ_k .

For the k th component, \mathbf{m}_k defines its center, σ_k specifies its minimum value (i.e., $f(\mathbf{m}_k)$), and \mathbf{H}_k is a $d \times d$ diagonal matrix whose principal diagonal elements affect the heights of the basin associated with the k th component across different dimensions. Further, \mathbf{R}_k serves as the rotation matrix for the k th component, and λ_k quantifies the linearity degree in its basin of attraction. The $\min(\cdot)$ function delineates the basins of attraction for each component.

Finally, $\mathbb{T}_k(\mathbf{a}) \mapsto \mathbf{b}$ is a non-linear transformation function [6] that introduces additional complexities to the basin of each component. This transformation function maps each element $a_j \in \mathbf{a}$ to:

$$a_j \mapsto \begin{cases} \exp \left(\log(a_j) + \mu_{k,1} \left(\sin(\omega_{k,1} \log(a_j)) + \sin(\omega_{k,2} \log(a_j)) \right) \right) & \text{if } a_j > 0 \\ 0 & \text{if } a_j = 0, \\ -\exp \left(\log(|a_j|) + \mu_{k,2} \left(\sin(\omega_{k,3} \log(|a_j|)) + \sin(\omega_{k,4} \log(|a_j|)) \right) \right) & \text{if } a_j < 0 \end{cases} \quad (2)$$

where for the k th component, this transformation is guided by parameters μ_k and ω_k , which define the symmetry and morphology of local optima on the basin of the k th component.

The transformation function $\mathbb{T}_k(\cdot)$ operates in three distinct regimes based on the value of each element $a_j \in \mathbf{a}$

¹The MATLAB source code for the GNBG problem instance generator is available at [40]. Users can employ this code to generate custom problem instances as per their requirements.

- For $a_j > 0$: The transformation employs an exponential modulation to a_j which is controlled by $\mu_{k,1}$ and the frequency parameters $\omega_{k,1}$ and $\omega_{k,2}$.
- For $a_j = 0$: The value is mapped directly to zero, independent of any μ or ω parameters. This serves as an invariant point in the transformation space, ensuring that the minimum position \mathbf{m}_k of the k th component remains unaltered.
- For $a_j < 0$: The transformation mirrors the process applied to $a_j > 0$ but acts on the absolute value $|a_j|$ before negating it. This is dictated by the parameters $\mu_{k,2}$, $\omega_{k,3}$, and $\omega_{k,4}$.

B. Parameter Sensitivity and Influence Analysis

In this section, we conduct an in-depth analysis of the parameters in GNBG, supported by illustrative examples. Understanding how these parameters influence the morphology, complexity, and behavior of the landscape is crucial for effectively configuring GNBG to create customized problem instances that align with specific research objectives.

To better understand the influence of GNBG's various parameters, we start by simplifying the model to a more basic, unimodal form. This involves neutralizing certain parameters and transformations. Specifically, we focus on the parameters o , μ , and ω , which dictate the modality of the landscape.

To generate a unimodal landscape, we set $o = 1$, indicating that the landscape is constructed from a single component. In this configuration, the $\min(\cdot)$ function in GNBG's original equation becomes redundant and can be omitted.

Next, to make the component unimodal, we set elements in vectors μ and ω to zero. This effectively neutralizes the transformation \mathbb{T} in equation (2). As a result, Equation (2) simplifies to:

$$a_j \mapsto \begin{cases} \exp(\log(a_j)) & \text{if } a_j > 0 \\ 0 & \text{if } a_j = 0 \\ -\exp(\log(|a_j|)) & \text{if } a_j < 0 \end{cases}, \quad (3)$$

which essentially becomes an identity mapping $a_j \mapsto a_j$. Therefore, we can omit the transformation \mathbb{T} in the GNBG's function in this case.

With these adjustments, GNBG's baseline function is rewritten as:

$$f(\mathbf{x}) = \sigma + ((\mathbf{R}(\mathbf{x} - \mathbf{m}))^\top \mathbf{H} \mathbf{R}(\mathbf{x} - \mathbf{m}))^\lambda. \quad (4)$$

In this simplified form, GNBG can only generate unimodal problem instances with \mathbf{m} and σ representing the global optimum position and value, respectively.

To further simplify GNBG, we set \mathbf{H} and \mathbf{R} to $\mathbf{I}_{d \times d}$. Setting matrices \mathbf{H} and \mathbf{R} to the identity matrix neutralizes their impact on the problem landscape. In fact, an identity matrix when used in linear transformations effectively preserves the vectors it multiplies. That is, any vector \mathbf{x} multiplied by an identity matrix remains \mathbf{x} . Therefore, setting \mathbf{H} and \mathbf{R} to $\mathbf{I}_{d \times d}$ means that they no longer modify the landscape in any way, as their multiplicative action becomes a 'do-nothing' operation. In this case, we can omit these matrices from GNBG's formulation. In addition, we set $\sigma = 0$ and $\mathbf{m} = \{m_i = 0 \mid i = 1, 2, \dots, d\}$ to neutralize their impact and removing them from GNBG's formulation. Therefore, using this configuration, GNBG's baseline can be rewritten as its simplest form:

$$f(\mathbf{x}) = (\mathbf{x}^\top \mathbf{x})^\lambda. \quad (5)$$

Now, we start by analyzing the impact of λ on the morphology of the component. The value of λ primarily dictates the linearity of the component's basin:

- To achieve a linear basin, λ must be set to 0.5.
- For $0 < \lambda < 0.5$ the generated component has a sub-linear basin. Very small values of this parameter will result in a needle-like morphology.
- For $\lambda > 0.5$, the component features a super-linear basin.

As illustrated in Figure 1, the value of λ affects the rate at which the basin of the component increases as it moves away from the center of the component. Therefore, the maximum function value in the problem space decreases or increases when we decrease or increase λ values, respectively.

Figures 1(a) to 1(c) compare the effect of increasing λ from 0.25 to 1 on the shape of the component's basin. It is worth mentioning that Equation (5) can be rewritten as $(\sum_{i=1}^d x_i^2)^\lambda$. Hence, if λ is set to one (see Figure 1(c)), GNBG resembles the Sphere function.

Next, we investigate the impact of elements of the principal diagonal of \mathbf{H} . In equation (5), the impact of \mathbf{H} was eliminated by setting it to $\mathbf{I}_{d \times d}$. By reintroducing \mathbf{H} into equation (5), GNBG becomes:

$$f(\mathbf{x}) = (\mathbf{x}^\top \mathbf{H} \mathbf{x})^\lambda. \quad (6)$$

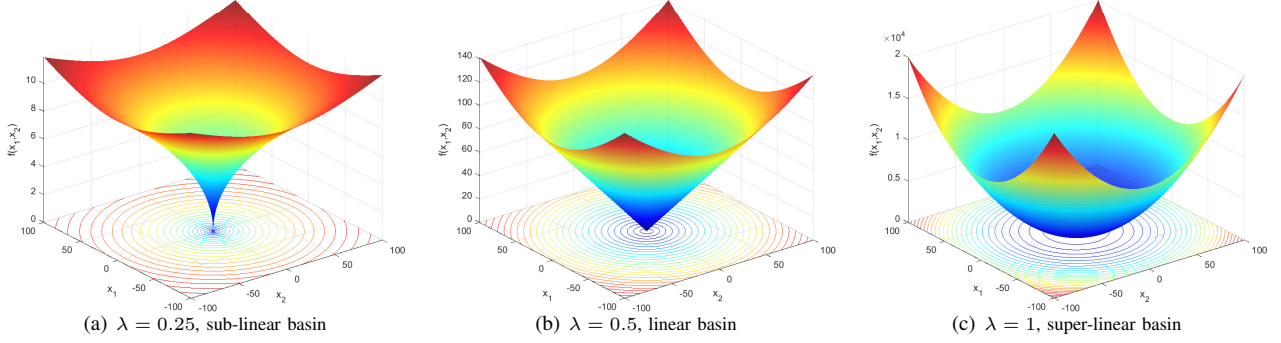


Fig. 1: Impact of λ values on the morphology of a component generated by GNBG. For these illustrative examples, we set $d = 2$, $o = 1$, $\boldsymbol{\mu} = (0, 0)$, $\boldsymbol{\omega} = (0, 0, 0, 0)$, $\sigma = 0$, $\mathbf{m} = (0, 0)$, $\mathbf{H} = \mathbf{I}_{2 \times 2}$, and $\mathbf{R} = \mathbf{I}_{2 \times 2}$. Additionally, the 2-dimensional problem space is bounded to $[-100, 100]$ in each dimension. For a component generated by GNBG, $\lambda < 0.5$ yields a sub-linear basin, $\lambda = 0.5$ yields a linear basin, and $\lambda > 0.5$ yields a super-linear basin.

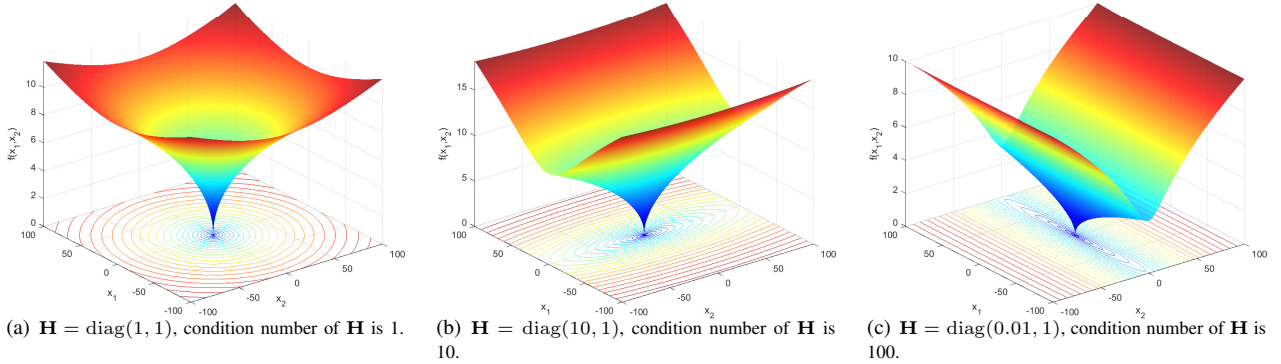


Fig. 2: Impact of \mathbf{H} values on the morphology of a component generated by GNBG. For these illustrative examples, we set $d = 2$, $o = 1$, $\boldsymbol{\mu} = (0, 0)$, $\boldsymbol{\omega} = (0, 0, 0, 0)$, $\sigma = 0$, $\mathbf{m} = (0, 0)$, $\lambda = 0.25$, and $\mathbf{R} = \mathbf{I}_{2 \times 2}$. Additionally, the 2-dimensional problem space is bounded to $[-100, 100]$ in each dimension.

\mathbf{H} is a $d \times d$ diagonal matrix, i.e., $\mathbf{H} = \text{diag}(h_1, h_2, \dots, h_d) \in \mathbb{R}^{d \times d}$, where $h_i = \mathbf{H}(i, i)$. The principal diagonal elements of \mathbf{H} serve to scale the heights of the component's basin across different dimensions. Equation (6) can be rewritten as $\left(\sum_{i=1}^d h_i x_i^2\right)^\lambda$, which indicates that the basin of the component along the i th dimension is scaled by a factor of h_i^λ .

Furthermore, \mathbf{H} influences the condition number of the component. The condition number of \mathbf{H} is defined as the ratio of its largest value to its smallest value among its principal diagonal elements, i.e., $\frac{\max_i |h_i|}{\min_i |h_i|}$. The condition number of \mathbf{H} directly affects the condition number of the component; however, its effect can be either amplified or dampened by the value of λ . It is worth mentioning that in Equation (6), if λ is set to one, and each element $\mathbf{H}(i, i)$ is set to $10^{\frac{i-1}{d-1}}$, GNBG resembles the Ellipsoidal function.

Figures 2(a), 2(b), and 2(c) illustrate how varying the values of \mathbf{H} affects the characteristics of the component's basin. In Figure 2(a), the principal diagonal elements of \mathbf{H} have identical values, resulting in a well-conditioned basin. In contrast, the \mathbf{H} matrices used to generate Figures 2(b) and 2(c) are ill-conditioned, resulting in basins that are likewise ill-conditioned.

In Equation (6), we assumed $\mathbf{R} = \mathbf{I}_{d \times d}$, so we could remove it from the baseline of GNBG. If we set \mathbf{R} to a non-identity orthogonal matrix, we need to add it to equation (6), which can be shown as:

$$f(\mathbf{x}) = ((\mathbf{R}\mathbf{x})^\top \mathbf{H} \mathbf{R}\mathbf{x})^\lambda. \quad (7)$$

\mathbf{R} is used for rotating the basin of the component. Considering the formulation of GNBG, the rotation is centered around the component without altering its minimum position. The rotation affects the variable interactions in the basin of a component. The introduction of a non-identity orthogonal rotation matrix \mathbf{R} for this component serves to rotate its basin. In GNBG, the role of the rotation matrix \mathbf{R} is pivotal for introducing complex variable interactions while preserving the original morphological traits of the component, such as its scale, height, and shape.

In GNBG, Givens rotation matrices are employed for their ability to allow targeted, customizable variable interactions. Unlike general orthogonal matrices that affect all variables simultaneously in a less controllable manner, Givens matrices

enable precise adjustments in the relationships between selected pairs of variables. This feature is particularly useful where we might need to fine-tune specific variable interactions without altering the entire variable interaction structure. The ability to focus on specific pairs of variables gives us a powerful tool for creating complex but comprehensible optimization landscapes. Further details on how these matrices are used to construct the global rotation matrix \mathbf{R} will be discussed later.

In cases where a component is not rotationally invariant –that is, it depends on the orientation of variables– we can modify the interaction between variable pairs using Givens rotation matrices. A Givens rotation matrix in a two-dimensional space is expressed as:

$$\mathbf{G} = \begin{pmatrix} \cos(\theta) & -\sin(\theta) \\ \sin(\theta) & \cos(\theta) \end{pmatrix}. \quad (8)$$

This matrix performs a rotation of angle θ in a plane defined by two coordinate axes. Extending this to higher dimensions, a Givens rotation matrix can selectively rotate variables within any two-dimensional subspace spanned by a pair of axes, while keeping all other dimensions unchanged. Therefore, to alter the variable interaction between each pair of variables p and q , we can construct the matrix as follows:

$$\mathbf{G}[i, j] = \begin{cases} 1 & \text{if } i = j \wedge i, j \neq p \wedge i, j \neq q \\ \cos(\theta) & \text{if } i = j = p \vee i = j = q \\ -\sin(\theta) & \text{if } i = p \wedge j = q \\ \sin(\theta) & \text{if } i = q \wedge j = p \\ 0 & \text{otherwise} \end{cases}. \quad (9)$$

For example, consider a Givens rotation matrix designed to modify the interaction between the third and seventh variables in an 8-dimensional space. The matrix takes the form:

$$\mathbf{G} = \begin{pmatrix} 1 & 0 & 0 & 0 & 0 & 0 & 0 & 0 \\ 0 & 1 & 0 & 0 & 0 & 0 & 0 & 0 \\ 0 & 0 & \cos(\theta_{3,7}) & 0 & 0 & 0 & -\sin(\theta_{3,7}) & 0 \\ 0 & 0 & 0 & 1 & 0 & 0 & 0 & 0 \\ 0 & 0 & 0 & 0 & 1 & 0 & 0 & 0 \\ 0 & 0 & 0 & 0 & 0 & 1 & 0 & 0 \\ 0 & 0 & \sin(\theta_{3,7}) & 0 & 0 & 0 & \cos(\theta_{3,7}) & 0 \\ 0 & 0 & 0 & 0 & 0 & 0 & 0 & 1 \end{pmatrix} \quad (10)$$

By setting θ to non-zero values, we can qualitatively change the variable interaction between variables p and q . Setting $\theta = 0$ keeps the Givens rotation matrix as the identity matrix $\mathbf{I}_{d \times d}$, which means the variable interaction between the p th and q th variables remains unaltered. The choice of θ can be used to modulate the ‘strength’ of interaction between each pair of variables. Specifically, setting θ to values away from the main axes (i.e., $k\frac{\pi}{2}, k \in \mathbb{Z}$) leads to stronger interactions. For instance, $\theta = \frac{\pi}{4}$ results in a more significant variable interaction compared to $\theta = \frac{\pi}{20}$.

To construct the complete rotation matrix \mathbf{R} , we first define an interaction matrix Θ for each component. This $d \times d$ matrix has all elements on and below the principal diagonal set to zero. Each element above the diagonal in the p th row and q th column ($\Theta(p, q)$) contains an angle, denoted as $\Theta(p, q)$ (where $p < q$). This angle sets the extent of rotation applied to the projection of \mathbf{x} in the basin of attraction of the k th component onto the plane $x_p - x_q$. After defining Θ , we employ Algorithm 1 to compute the final rotation matrix \mathbf{R} for the component.

Algorithm 1 generates a rotation matrix, denoted as \mathbf{R}_k , that rotates the projection of \mathbf{x} within the basin of attraction of the k th component based on a given matrix Θ_k . By setting $\Theta_k(p, q)$ to values that are not multiples of $\frac{\pi}{2}$ (i.e., non-axis-overlapped values), we establish variable interactions between p and q . The strength of this interaction is determined by how far $\Theta_k(p, q)$ deviates from multiples of $\frac{\pi}{2}$. For example, a $\Theta_k(p, q)$ value of $\frac{\pi}{4}$ would induce a strong variable interaction, while a value close to $\frac{\pi}{180}$ would result in weaker interactions. Setting $\Theta_k(p, q)$ to zero ensures that \mathbf{R}_k does not modify the interaction between p th and q th variables.

Therefore, Algorithm 1 can generate various types of variable interaction structures, ranging from different degrees of separability, depending on the values included in Θ_k . It should be noted that \mathbf{R}_k can be used to alter variable interaction when the k th component is rotation-dependent². Moreover, for generating partially separable components, it is crucial to ensure they are originally fully separable and rotation-dependent.

This approach provides an intuitive and flexible way to control variable interactions in each component. By storing the rotation angles between variable pairs in a matrix Θ_k , we gain a straightforward yet powerful means to manipulate each

²GNBG is capable of generating rotation-invariant components.

Algorithm 1: Pseudo code for calculating the rotation matrix \mathbf{R}_k based on Θ_k .

Input: d and Θ_k

Output: \mathbf{R}_k

```

1  $\mathbf{R}_k = \mathbf{I}_{d \times d}$ ;
2 for  $p = 1$  to  $d - 1$  do
3   for  $q = p + 1$  to  $d$  do
4     if  $\Theta_k(p, q) \neq 0$  then
5        $\mathbf{G} = \mathbf{I}_{d \times d}$ ;
6        $\mathbf{G}(p, p) = \cos(\Theta_k(p, q))$ ; //  $\Theta_k(a, b)$  and  $\mathbf{G}(a, b)$  are the elements at  $a$ th row and  $b$ th column of
          matrices  $\Theta_k$  and  $\mathbf{G}$ , respectively.
7        $\mathbf{G}(q, q) = \cos(\Theta_k(p, q))$ ;
8        $\mathbf{G}(p, q) = -\sin(\Theta_k(p, q))$ ;
9        $\mathbf{G}(q, p) = \sin(\Theta_k(p, q))$ ;
10       $\mathbf{R}_k = \mathbf{R}_k \times \mathbf{G}$ ; //  $\mathbf{G}$  is the Givens rotation matrix for  $x_p - x_q$  plane based on  $\Theta_k(p, q)$ .
11 Return  $\mathbf{R}_k$ ;
```

component's variable interaction. Coupled with the selective nature of Givens rotations, this strategy offers fine-grained control over the structure of each component's basin of attraction, thereby allowing us to create complex but analytically tractable landscapes.

In Figure 3, we demonstrate several examples illustrating how different configurations of Θ can be used to generate various variable interaction structures within an 8-dimensional component. We assume that the component is initially fully-separable and rotation-dependent. In each example, $\Theta_k(p, q) = \theta_{p,q}$ is set to a value that is not a multiple of $\frac{\pi}{2}$ (i.e., $\Theta_k(p, q) \neq k\frac{\pi}{2}, k \in \mathbb{Z}$). Additionally, we provide a variable interaction graph for each Θ matrix. In these graphs, an edge exists between vertices p and q if $\Theta_k(p, q) = \theta_{p,q}$ is both non-zero and not a multiple of $\frac{\pi}{2}$.

Besides manually configuring Θ for specific desired variable interaction structures, GNBG also allows for the generation of components with random variable interaction structures and strengths. To achieve this, we introduce a parameter \mathfrak{p} to represent the probability of each element above the principal diagonal in Θ being either zero or a randomly generated angle. For each $\Theta_k(p, q)$, a random number is generated from a uniform distribution. If this number is less than or equal to \mathfrak{p} , then $\Theta_k(p, q)$ is set to zero ($q > p$). Otherwise, it is set to a random angle in the range $(0, 2\pi)$. Smaller values of \mathfrak{p} result in variable interaction structures with fewer connections between variables, while larger values generate more complex structures with increased connectivity. Setting \mathfrak{p} to zero or one yields fully separable and fully connected variable interaction structures, respectively. Users may also choose to randomly assign angles from a predefined set of values based on \mathfrak{p} rather than generating them in a continuous range.

Figure 4 illustrates how rotation affects the basin of attraction for a given component when \mathbf{R} is generated using Algorithm 1 with a user-defined angle. To facilitate visualization, we set $d = 2$. In this case, there is only a single plane $x_1 - x_2$, and the output of Algorithm 1 corresponds to equation (8).

Now we analyze the influence of the $\boldsymbol{\mu}$ and $\boldsymbol{\omega}$ parameters in the transformation \mathbb{T} . By setting $\boldsymbol{\mu}$ and $\boldsymbol{\omega}$ to non-zero values, the transformation \mathbb{T} in equation (2) is enabled and reintroduced to Equation (7), which changes the formulation to:

$$f(\mathbf{x}) = (\mathbb{T}((\mathbf{R}\mathbf{x})^\top) \mathbf{H} \mathbb{T}(\mathbf{R}\mathbf{x}))^\lambda. \quad (11)$$

By setting the elements of $\boldsymbol{\mu}$ and $\boldsymbol{\omega}$ to non-zero values, we induce the formation of local optima within the component's basin. In this transformation, sinusoidal functions are utilized to create irregularities and local optima, and the values of $\boldsymbol{\mu}$ and $\boldsymbol{\omega}$ determine the size, morphology, and symmetry of these local optima. Specifically:

- The $\boldsymbol{\mu}$ parameters control the amplitude of the sinusoidal components, affecting the depth of local optima. Different values of $\mu_{k,1}$ and $\mu_{k,2}$ introduce asymmetric non-linearity, leading to asymmetry in the basin.
- The $\boldsymbol{\omega}$ parameters dictate the frequency of the sinusoidal functions, affecting the number and vastness of the local optima. Varied $\boldsymbol{\omega}$ values add complexity to the transformation by changing the frequency of oscillations. $\boldsymbol{\omega}$ values affect the frequency of oscillations introduced by the sinusoidal functions. Moreover, asymmetric patterns in the basins can be introduced through different settings for $\omega_1, \omega_2, \omega_3$, and ω_4 .

Consequently, by adjusting $\boldsymbol{\mu}$ and $\boldsymbol{\omega}$, the characteristics of the transformed space can be manipulated, thus affecting the landscape in various ways. Figure 5 consists of nine plots that illustrate the impact of $\boldsymbol{\mu}$ and $\boldsymbol{\omega}$ on the local optima surrounding the component. In each plot, we consider a scenario with $o = 1$ representing a scenario with a single component, $\lambda = 0.25$, $\sigma = 0$, and $\mathbf{m}=(0,0)$. To isolate the impact of the transformation, $\mathbf{H} = \mathbf{R} = \mathbf{I}_{d \times d}$. Therefore, equation (11) simplifies to $f(\mathbf{x}) = (\mathbb{T}(\mathbf{x}^\top) \mathbb{T}(\mathbf{x}))^\lambda$.

$$\Theta = \begin{pmatrix} 0 & 0 & 0 & 0 & 0 & 0 & 0 & 0 \\ 0 & 0 & 0 & 0 & 0 & 0 & 0 & 0 \\ 0 & 0 & 0 & 0 & 0 & 0 & 0 & 0 \\ 0 & 0 & 0 & 0 & 0 & 0 & 0 & 0 \\ 0 & 0 & 0 & 0 & 0 & 0 & 0 & 0 \\ 0 & 0 & 0 & 0 & 0 & 0 & 0 & 0 \\ 0 & 0 & 0 & 0 & 0 & 0 & 0 & 0 \\ 0 & 0 & 0 & 0 & 0 & 0 & 0 & 0 \end{pmatrix}$$

(a) All angles are set to zero. This configuration does not alter any variable interaction.

$$\Theta = \begin{pmatrix} 0 & \theta_{1,2} & \theta_{1,3} & \theta_{1,4} & \theta_{1,5} & \theta_{1,6} & \theta_{1,7} & \theta_{1,8} \\ 0 & 0 & \theta_{2,3} & \theta_{2,4} & \theta_{2,5} & \theta_{2,6} & \theta_{2,7} & \theta_{2,8} \\ 0 & 0 & 0 & \theta_{3,4} & \theta_{3,5} & \theta_{3,6} & \theta_{3,7} & \theta_{3,8} \\ 0 & 0 & 0 & 0 & \theta_{4,5} & \theta_{4,6} & \theta_{4,7} & \theta_{4,8} \\ 0 & 0 & 0 & 0 & 0 & \theta_{5,6} & \theta_{5,7} & \theta_{5,8} \\ 0 & 0 & 0 & 0 & 0 & 0 & \theta_{6,7} & \theta_{6,8} \\ 0 & 0 & 0 & 0 & 0 & 0 & 0 & \theta_{7,8} \\ 0 & 0 & 0 & 0 & 0 & 0 & 0 & 0 \end{pmatrix}$$

(c) All angles are set to values that are not a multiple of $\frac{\pi}{2}$, resulting in a fully non-separable fully-connected variable interaction structure.

$$\Theta = \begin{pmatrix} 0 & \theta_{1,2} & 0 & 0 & 0 & 0 & 0 & 0 \\ 0 & 0 & \theta_{2,3} & 0 & 0 & 0 & 0 & 0 \\ 0 & 0 & 0 & \theta_{3,4} & 0 & 0 & 0 & 0 \\ 0 & 0 & 0 & 0 & \theta_{4,5} & 0 & 0 & 0 \\ 0 & 0 & 0 & 0 & 0 & \theta_{5,6} & 0 & 0 \\ 0 & 0 & 0 & 0 & 0 & 0 & \theta_{6,7} & 0 \\ 0 & 0 & 0 & 0 & 0 & 0 & 0 & \theta_{7,8} \\ 0 & 0 & 0 & 0 & 0 & 0 & 0 & 0 \end{pmatrix}$$

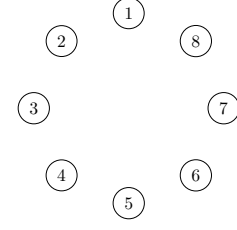
(e) A non-separable structure with the minimum number of variable interactions. There is an interaction only between i th and $(i+1)$ th variables.

$$\Theta = \begin{pmatrix} 0 & \theta_{1,2} & \theta_{1,3} & \theta_{1,4} & 0 & 0 & 0 & 0 \\ 0 & 0 & \theta_{2,3} & \theta_{2,4} & 0 & 0 & 0 & 0 \\ 0 & 0 & 0 & \theta_{3,4} & 0 & 0 & 0 & 0 \\ 0 & 0 & 0 & 0 & 0 & 0 & 0 & 0 \\ 0 & 0 & 0 & 0 & 0 & \theta_{5,6} & \theta_{5,7} & \theta_{5,8} \\ 0 & 0 & 0 & 0 & 0 & 0 & \theta_{6,7} & \theta_{6,8} \\ 0 & 0 & 0 & 0 & 0 & 0 & 0 & \theta_{7,8} \\ 0 & 0 & 0 & 0 & 0 & 0 & 0 & 0 \end{pmatrix}$$

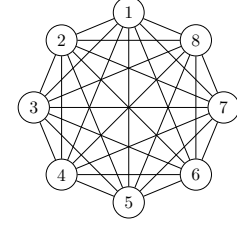
(g) Θ is configured to create a partially separable variable interaction structure with two fully connected groups of variables.

$$\Theta = \begin{pmatrix} 0 & \theta_{1,2} & 0 & 0 & 0 & 0 & 0 & 0 \\ 0 & 0 & 0 & 0 & 0 & 0 & 0 & 0 \\ 0 & 0 & 0 & 0 & 0 & 0 & 0 & 0 \\ 0 & 0 & 0 & 0 & \theta_{4,5} & \theta_{4,6} & \theta_{4,7} & 0 \\ 0 & 0 & 0 & 0 & 0 & \theta_{5,6} & 0 & 0 \\ 0 & 0 & 0 & 0 & 0 & 0 & \theta_{6,7} & 0 \\ 0 & 0 & 0 & 0 & 0 & 0 & 0 & 0 \\ 0 & 0 & 0 & 0 & 0 & 0 & 0 & 0 \end{pmatrix}$$

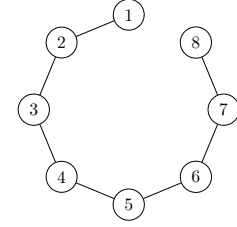
(i) Θ is set to create a variable interaction structure containing two separable variables x_3 and x_8 , a pair of connected variables $\{x_1, x_2\}$, and a group of connected (not fully-connected) variables $\{x_4, x_5, x_6, x_7\}$.



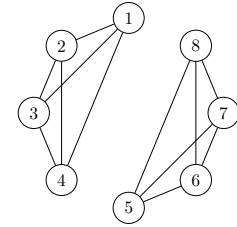
(b) Fully disconnected variable interaction graph.



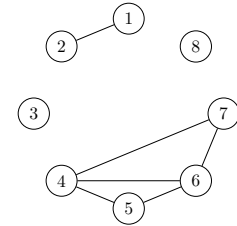
(d) Fully connected variable interaction graph.



(f) A chain-like connected variable interaction graph.



(h) A disconnected graph with two fully-connected sub-graphs.



(j) A disconnected variable interaction graph with two groups of variables and two separable variables.

Fig. 3: Examples of how, by configuring Θ , GNBG can generate desired variable interaction structures in an 8-dimensional component. Note that the component must be originally fully-separable and rotation-dependent. The variable interaction graphs associated with each matrix Θ are illustrated in the right column.

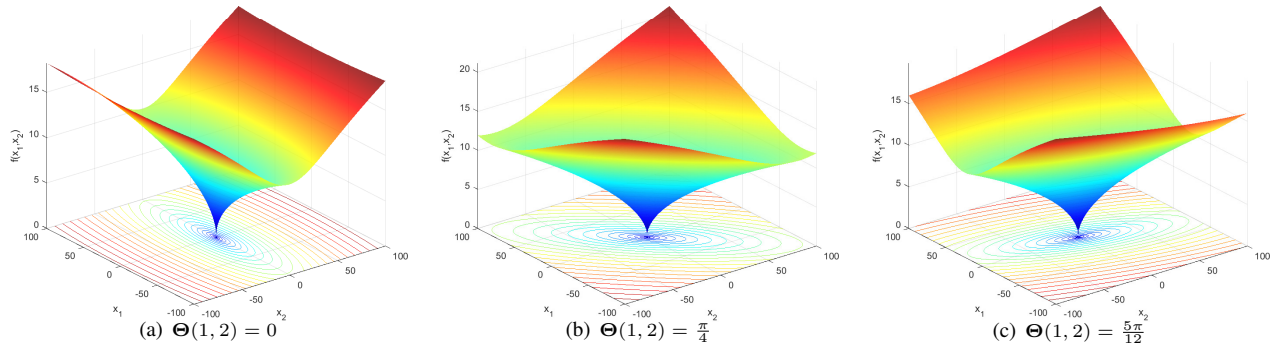


Fig. 4: Impact of rotating the projection of \mathbf{x} in the basin of a component onto the x_1 - x_2 plane with different angles $\Theta(1,2)$. For generating these illustrative examples, we set $d = 2$, $o = 1$, $\boldsymbol{\mu} = (0,0)$, $\boldsymbol{\omega} = (0,0,0,0)$, $\sigma = 0$, $\mathbf{m} = (0,0)$, $\lambda = 0.25$, $\mathbf{H} = \text{diag}(1,10)$, and \mathbf{R} is obtained by Algorithm 1 based on the given angle $\Theta(1,2)$. Additionally, the 2-dimensional problem space is bounded to $[-100,100]$ in each dimension.

The plots in Figures 5(a) to 5(c) correspond to different $\boldsymbol{\omega}$ values while keeping $\boldsymbol{\mu} = (0.2, 0.2)$ constant. We observe that increasing $\boldsymbol{\omega}$ values leads to an increase in the number of local optima within the basin, while also reducing their width.

Comparing the plots in Figures 5(d) to 5(e) offers insights into the influence of $\boldsymbol{\mu}_k$ on the local optima within the basin. In these plots, $\boldsymbol{\omega}$ is set to $(50,50,50,50)$. From Figures 5(a) to 5(e), we observe that while $\boldsymbol{\mu}$ impacts the amplitude and thus the depth of the local optima—without affecting their number or width—it is worth noting that $\boldsymbol{\omega}$ exclusively influences the frequency and spatial distribution of these optima. Specifically, variations in $\boldsymbol{\omega}$ values do not affect the depth of the local optima but do alter their number and width within the basin. Furthermore, higher $\boldsymbol{\mu}_k$ values lead to increased heights for the basin local optima, consequently elevating the height of the basin surrounding the component.

In each of the plots presented in Figures 5(a) to 5(e), symmetric components are depicted, with $\mu_1 = \mu_2$ and $\omega_1 = \omega_2 = \omega_3 = \omega_4$. To introduce asymmetry into the components, one can assign distinct values to the elements of $\boldsymbol{\mu}_k$, such that $\mu_1 \neq \mu_2$. It is important to note that the degree of asymmetry in the depth of local optima increases with larger discrepancies between the values of the $\boldsymbol{\mu}_k$ elements. Similarly, setting distinct values for the elements of $\boldsymbol{\omega}$ can introduce asymmetric characteristics in the frequency and spatial distribution of local optima. Figures 5(g) to 5(i) demonstrate the impact of varying the values of $\boldsymbol{\mu}$ and $\boldsymbol{\omega}$ in creating asymmetrical characteristics.

Up to this point, we have set $\sigma = 0$ and $\mathbf{m} = \{m_i = 0 \mid i = 1, 2, \dots, d\}$ to neutralize the impact of these parameters in GNBG. This choice resulted in positioning the minimum (or base) of the component at $[0, 0, \dots, 0] \in \mathbb{R}^{1 \times d}$ and making its minimum function value equal to zero. In GNBG, the σ_k and \mathbf{m}_k parameters can be utilized to specify the minimum function value and the position of the k th component, respectively. Incorporating σ and \mathbf{m} into equation (11), we get:

$$f(\mathbf{x}) = \sigma + (\mathbb{T}(\mathbf{R}(\mathbf{x} - \mathbf{m}))^\top) \mathbf{H} \mathbb{T}(\mathbf{R}(\mathbf{x} - \mathbf{m})), \quad (12)$$

which represents the complete form of GNBG for generating a single component. Here, σ_k and \mathbf{m}_k serve to translate (or shift) the minimum of the k th component in the objective space and the solution space, respectively. By manipulating \mathbf{m}_k values, users can precisely define the minimum positions of the components. In GNBG, $f(\mathbf{m}_k) = \sigma_k$ determines the minimum value of the k th component. Importantly, altering σ_k does not affect the morphology of the component but merely shifts its basin in the objective space, effectively shifting the function values across the entire basin of the component.

The next parameter of GNBG is o , which defines the number of components in the search space. By setting $o = 1$ in equation (12), we removed the impact of this parameter. By setting the value of o to be larger than one, equation (12) extends to (1), resulting in a problem space that includes multiple components, each with its own basin defined by the $\min(\cdot)$ function in (1). Each component k in GNBG has its own parameter settings, and the only parameter that all components share is the dimension. Therefore, these components are independent of each other and can exhibit different characteristics based on their parameter settings. The minimum position of the component with the smallest σ value corresponds to the global optimum position. Furthermore, the objective value of the global optimum is equal to the smallest σ value among all components.

Note that increasing the number of components directly impacts the computational complexity of function evaluations. For instance, evaluating the objective value of a candidate solution in a 30-dimensional problem instance with 10 components takes approximately twice as long as an objective function evaluation in a 30-dimensional problem instance with five components.

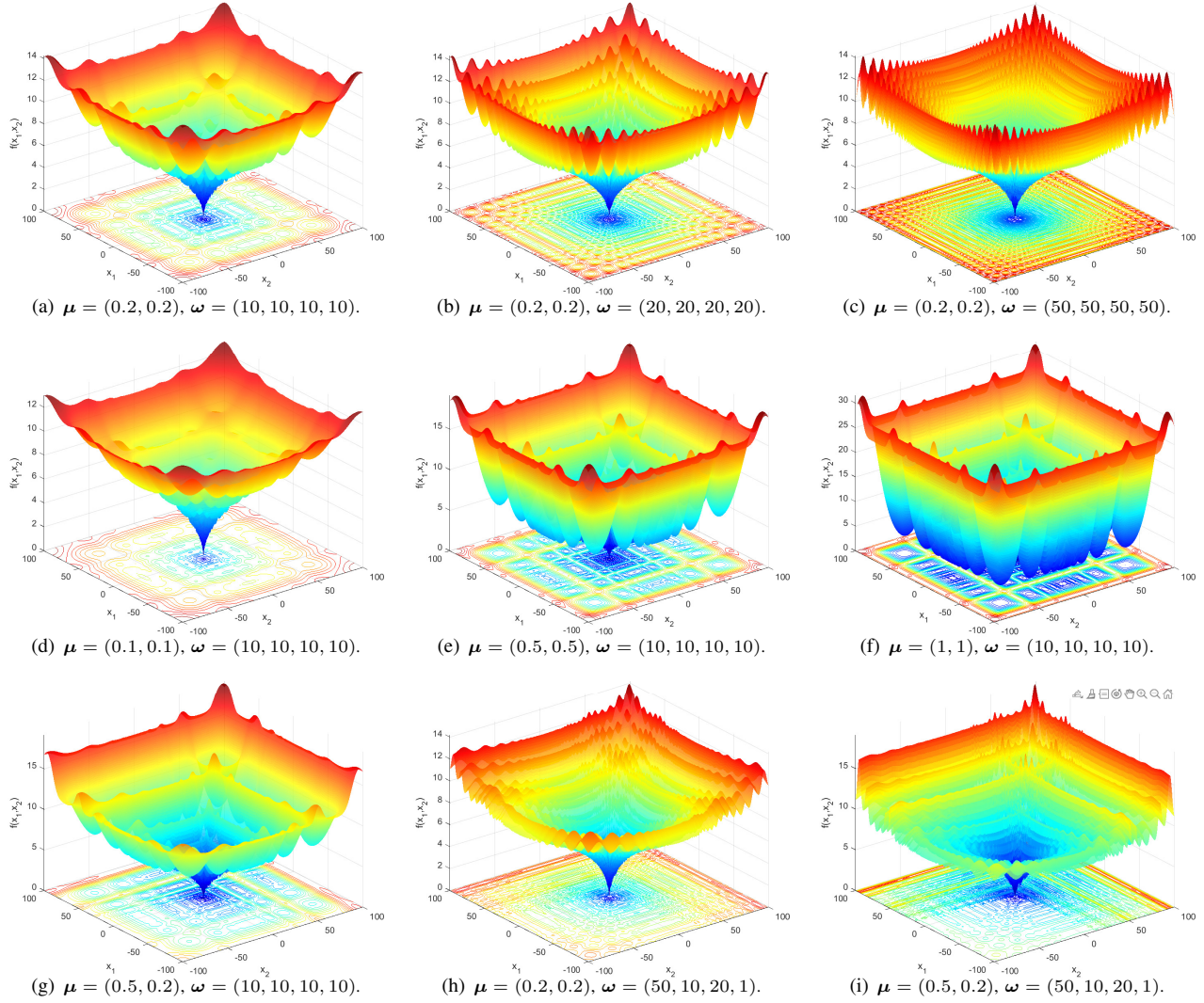


Fig. 5: Impact of μ and ω values on a 2-dimensional component generated by GNBG. For these illustrative examples, the 2-dimensional problem space is bounded to $[-100, 100]$ in each dimension, $o = 1$, $\sigma = 0$, $\mathbf{m} = (0, 0)$, $\lambda = 0.25$, $\mathbf{H} = \text{diag}(1, 1)$, and $\mathbf{R} = \mathbf{I}_{2 \times 2}$.

Figure ?? illustrates three problem instances each possessing multiple components. In these instances, the value of o is set to $\{2, 10, 50\}$. We have employed simple unimodal components in these illustrations to highlight the effects of using multiple components without the interference of other morphological traits. Notably, the count of discernible components in Figures 6(b) and 6(c) is less than the specified values of o for each landscape. This discrepancy is a significant factor to consider when designing problem instances with multiple components, especially when some of parameters are generated randomly. For these figures, the parameters σ_k , \mathbf{m}_k , and \mathbf{H}_k are generated randomly. There exists the potential for some components to be overshadowed or ‘dominated’ by the basins of larger components. By ‘dominated’, we imply that these components might not significantly influence the search space but might add to the computational complexity. A strategy to pinpoint such dominated components is by evaluating the function value at each component’s minimum position. If the condition $f(\mathbf{m}_k) < \sigma_k$ holds for the k th component, it signals that the component is ensnared and dominated by other components’ basins.

Finally, we discuss the role of the dimensionality parameter d in GNBG. The GNBG is designed to be scalable with respect to dimensionality. As d increases, the complexity of the search space correspondingly grows, making the optimization problem increasingly challenging to navigate. Higher values for d not only inflate the computational burden but may also exacerbate the ‘curse of dimensionality,’ also referred to as the ‘scalability issue,’ leading conventional optimization algorithms to perform suboptimally [28, 29]. Therefore, it is crucial to judiciously select the value of d , striking a balance between problem complexity and computational feasibility. Table I summarizes the parameters of GNBG.

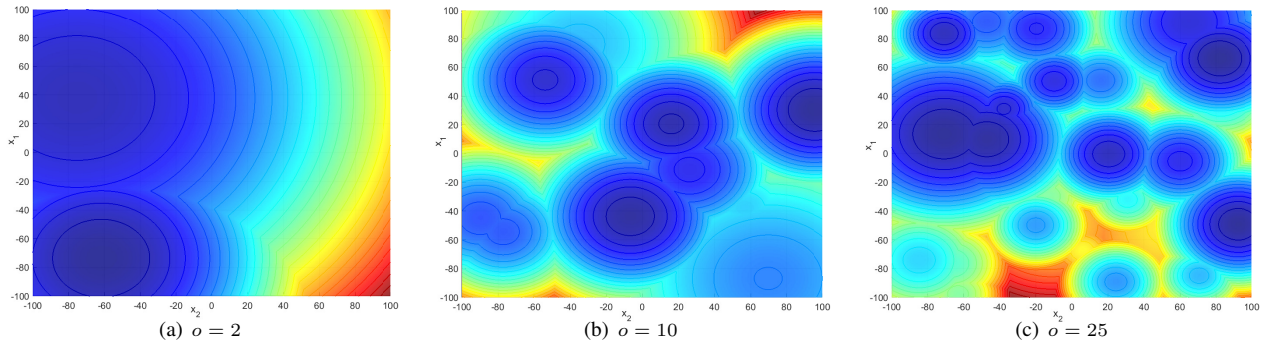


Fig. 6: Solution spaces produced by GNBG with multiple components. For these visualizations, we employed simplified component forms: we set λ_k to one, \mathbf{R} as the identity matrix, ensured well-conditioned components by setting $\mathbf{H}_k(1, 1) = \mathbf{H}_k(2, 2)$, and neutralized \mathbb{T} by setting all elements of $\boldsymbol{\mu}_k$ and $\boldsymbol{\omega}_k$ to zero. Moreover, σ_k values were randomly selected from the interval $[0,10]$, \mathbf{H}_k values from $[0.001,0.01]$, and the minimum position for each component, \mathbf{m}_k , from $[-100,100]$.

TABLE I: Summary of the parameters, functions, and notations used in GNBG.

Symbol	Description
$f(\cdot)$	GNBG's baseline function.
d	Represents the number of components in the search space.
\mathbb{X}	d -dimensional search space.
\mathbf{x}	A d -dimensional solution (x_1, x_2, \dots, x_d) in the search space \mathbb{X} .
l_i	Lower bound of search range in the i th dimension.
u_i	Upper bound of search range in the i th dimension.
o	Number of components in the search space.
$\min(\cdot)$	Defines the basin of attraction of each component.
\mathbf{m}_k	Minimum position of the k th component.
σ_k	Minimum value of the k th component, i.e., $f(\mathbf{m}_k) = \sigma_k$.
\mathbf{H}_k	It is a $d \times d$ diagonal matrix, i.e., $\mathbf{H}_k = \text{diag}(h_1, h_2, \dots, h_d) \in \mathbb{R}^{d \times d}$, where $h_i = \mathbf{H}_k(i, i)$. The principal diagonal elements of \mathbf{H}_k are scaling factors that influence the heights of the basin associated with the k th component across different dimensions. Moreover, this matrix directly affect the condition number of the k th component.
\mathbf{R}_k	It is a $d \times d$ orthogonal matrix used for rotating the k th component.
Θ_k	It is a $d \times d$ matrix, whose elements are utilized to compute the rotation matrix \mathbf{R}_k by Algorithm 1. The elements on and below the principal diagonal of Θ_k are zero. An element located at the p th row and q th column of Θ_k , denoted as $\Theta_k(p, q)$, specifies the rotation angle for the plane x_p - x_q , where $p < q$. In essence, $\Theta_k(p, q)$ governs the interaction between variables $x_p, x_q \in \mathbf{x}$.
p_k	In cases where Θ_k is randomly generated, $0 \leq p_k \leq 1$ controls the random generation of elements above the principal diagonal in the Θ_k matrix. For each $\Theta_k(p, q)$ where $p < q$, a random number is drawn from a uniform distribution. If this number is less than or equal to p_k , $\Theta_k(p, q)$ is set to zero. Otherwise, $\Theta_k(p, q)$ is assigned a predefined or a random angle.
λ_k	It is a positive constant that affects the rate at which the basin of the k th component increases. The specific pattern can range from super-linear ($\lambda_k > 0.5$) to linear ($\lambda_k = 0.5$) to sub-linear ($0 < \lambda_k < 0.5$).
$\mathbb{T}(\cdot)$	An element-wise non-linear transformation that plays a role in controlling the modality, irregularity, roughness, and symmetry of each component. The specific characteristics of the k th component are determined by the values of $\boldsymbol{\mu}_k$ and $\boldsymbol{\omega}_k$ within the transformation function.
$\boldsymbol{\mu}_k$	The vector $\boldsymbol{\mu}_k$ consists of two elements, denoted as $\boldsymbol{\mu}_k = (\mu_{k,1}, \mu_{k,2})$. These elements play a crucial role in determining the depth of the local optima within the basin of the k th component. By assigning different values to $\mu_{k,1}$ and $\mu_{k,2}$, an asymmetry is introduced into the basin of the k th component.
$\boldsymbol{\omega}_k$	The vector $\boldsymbol{\omega}_k$ consists of four elements, denoted as $\boldsymbol{\omega}_k = (\omega_{k,1}, \omega_{k,2}, \omega_{k,3}, \omega_{k,4})$. Together with the $\boldsymbol{\mu}_k$ values, these elements play a significant role in shaping the characteristics of the "basin optima" within the basin of the k th component. The values of $\omega_{k,1}, \omega_{k,2}, \omega_{k,3}$, and $\omega_{k,4}$ contribute to determining the number and width of local optima within the basin of the k th component. Furthermore, differences between these elements impact the symmetry of the basin of the k th component.

III. PROBLEM INSTANCE GENERATION FOR SPECIFIC RESEARCH OBJECTIVES

In this section, we outline how to harness GNBG's configurability and flexibility for generating problem instances tailored to specific research objectives. By adjusting controllable problem characteristics within GNBG, researchers can construct instances that enable in-depth analysis of optimization algorithm performance. This comprehensive approach provides nuanced insights into an algorithm's strengths and weaknesses when faced with either individual or compounded problem characteristics—each of which can be controlled to varying degrees. In the rest of this section, we explore how to fine-tune GNBG's parameter settings to produce problem instances characterized by diverse basin linearity, conditioning, variable interaction structures, multi-modality, deceptiveness through existence of multiple competitive components, and various combinations of these characteristics.

A. Exploring Basin Linearity

In GNBG, the parameter λ_k serves as the determinant for the linearity of the basin associated with the k -th component. To rigorously assess how variations in basin linearity influence the performance of optimization algorithms, a systematic exploration of λ values is warranted. For a targeted analysis focusing solely on basin linearity, it is imperative to neutralize confounding factors such as multi-modality, variable interaction, and ill-conditioning. To accomplish this, the number of components o is set to one, thereby generating a single-component landscape. Further, the transformation \mathbb{T} is neutralized by setting all elements of vectors $\boldsymbol{\mu}$ and $\boldsymbol{\omega}$ to zero. We also set both \mathbf{H} and \mathbf{R} as identity matrices to generate well-conditioned and unrotated component.

With these settings in place, λ can be selectively manipulated to create problem instances designed to elucidate the impact of basin linearity on algorithmic performance. Values of λ less than 0.5 yield sub-linear basins, where the curvature around the optimal solution becomes increasingly narrow and acute as λ decreases. A λ value of 0.5 leads to a linear basin, while values greater than 0.5 result in super-linear basins. To comprehensively probe the influence of basin linearity, one may opt to set λ from a discrete set such as $\{0.1, 0.25, 0.5, 0.75, 1\}$. This facilitates a comparative analysis, allowing for insights into the relative merits and limitations of optimization algorithms in navigating basins with varying degrees of linearity.

B. Investigating various conditioning

Ill-conditioning is a characteristic frequently encountered in real-world optimization problems. Traditional approaches to studying algorithm robustness to ill-conditioning often rely on baseline functions with fixed condition numbers, such as the Ellipsoid function [6]. GNBG offers a more flexible alternative: by manipulating the condition number of \mathbf{H}_k , users can control the condition number of the k -th component. This flexibility allows for a more nuanced investigation into the robustness of optimization algorithms when faced with varying degrees of ill-conditioning.

To focus exclusively on the impact of ill-conditioning on the performance of algorithms, we neutralize other challenging characteristics. Specifically, we set the number of components o to one and neutralize the transformation \mathbb{T} by setting all elements of vectors $\boldsymbol{\mu}$ and $\boldsymbol{\omega}$ to zero to create a unimodal landscape. Additionally, λ is set to one, and \mathbf{R} is configured as an identity matrix to ensure a separable component.

For a comprehensive study, users can vary the condition number of \mathbf{H} across a wide range, such as $\{10, 10^2, \dots, 10^7\}$. To achieve specific condition number c , two randomly chosen elements of the diagonal of \mathbf{H} are set to a and b such that $b > a$ and $\frac{b}{a} = c$. Remaining diagonal elements are randomly sampled from the range $[a, b]$ according to a Beta distribution parameterized by $0 < \alpha = \beta \leq 1$. Here, $\alpha = \beta = 1$ approximates a uniform distribution, while smaller α and β values increase the likelihood of generating numbers closer to a or b .

C. Exploring Variable Interaction Structures

Real-world optimization problems exhibit a variety of variable interaction structures, ranging from fully separable to intricately connected, non-separable configurations [41]. GNBG offers considerable flexibility in generating desired variable interaction structures for each component k by manipulating the Θ_k matrix. While users have the option to manually configure Θ_k , GNBG also offers predefined settings that facilitate various degrees of separability and connection strengths, where the connectivity degree can be controlled through the parameter \mathfrak{p}_k in the range $[0, 1]$. A \mathfrak{p}_k value of 0 does not alter the variable interaction structure, whereas a value of 1 yields a fully connected, non-separable structure. Intermediate values of \mathfrak{p}_k can result in partially separable components characterized by varying degrees of inter-variable connections.

To isolate the influence of variable interaction structures on algorithmic performance, other confounding factors must be controlled. Here, we set the number of components o to one and vectors $\boldsymbol{\mu}$ and $\boldsymbol{\omega}$ to zero, to generate a unimodal landscape. The diagonal elements of \mathbf{H} are randomly generated from the uniform distribution in the range $[1, 100]$, yielding a maximum condition number of 100—a value we find (see Table III) to have a negligible impact on the performance of most algorithms. For a comprehensive evaluation, users can set \mathfrak{p}_k values across a wide range, such as $\{0, 0.25, 0.5, 0.75, 1\}$. Angles between variable pairs, randomly selected from the range $[-\pi, \pi]$. Angles closer to the axes imply weaker connections, while those deviating significantly from the axes yield stronger interactions. For more focused studies, these angles can be preset to specific values—such as $\frac{\pi}{4}$ and $\frac{5\pi}{180}$ —to explore the impact of strong and weak connections within a fully connected structure, respectively.

D. Exploring the Impact of Multimodality with various morphological characteristics

Real-world optimization landscapes frequently present numerous local optima, posing significant challenges to optimization algorithms susceptible to premature convergence. GNBG offers a robust mechanism for generating such intricate landscapes by utilizing the nonlinear transformation \mathbb{T} . Specifically, the geometry—width, depth, and multiplicity—of the local optima within the basin of attraction of each component k can be controlled through the vectors $\boldsymbol{\mu}_k$ and $\boldsymbol{\omega}_k$.

To focus on the ability of optimization algorithms to navigate landscapes with local optima of varying characteristics, we generate test instances devoid of other confounding elements like ill-conditioning and rotation. This is achieved by setting both \mathbf{H} and \mathbf{R} as identity matrices. Additionally, we set λ to one to maintain full separability of the multimodal landscape. Moreover, setting λ to one serves to obviate the complexities introduced by sub-linear basins. Although setting o to values greater than one typically results in multimodal instances, we restrict the problem to a single component by setting this parameter to one. This approach eliminates challenges associated with existence of multiple promising regions, which contribute to the deceptiveness of the problem instances. Finally, to achieve a symmetric distribution of local optima within the basin, we enforce $\mu_1 = \mu_2$ and $\omega_1 = \omega_2 = \omega_3 = \omega_4$.

For a rigorous evaluation, users are encouraged to vary $\boldsymbol{\mu}$ and $\boldsymbol{\omega}$ across a wide range, such as $\{0.1, 0.25, 0.5, 0.75, 1\}$ and $\{5, 25, 50, 100\}$, respectively. Lower values of $\boldsymbol{\mu}$ yield shallower local optima, while higher values deepen them. The $\boldsymbol{\omega}$ values modulate both the width and density of the local optima—higher values narrow the optima while increasing their multiplicity.

E. Exploring the Impact of Multiple Competitive Components

Many real-world optimization landscapes contain multiple promising regions, each characterized by vast basins of attraction surrounding high-quality solutions [42, 43]. These regions can mislead optimization algorithms, diverting them into suboptimal solutions. GNBG provides the flexibility to generate such intricate landscapes by allowing users to specify multiple components, each with its own set of attributes including position, size, and other morphological characteristics. Note that, incorporating multiple components imbues the landscape with a pronounced asymmetry. Furthermore, even when configuring \mathbf{R}_k as the identity matrix, the presence of multiple components inherently makes the problem instance fully non-separable [44].

To isolate the impact of multiple promising regions, we standardize certain component attributes. Specifically, we set $\lambda_k = 1$ for all components to maintain a uniformly scaled landscape. Additionally, we neutralize other influencing factors by setting all elements of $\boldsymbol{\mu}_k$ and $\boldsymbol{\omega}_k$ to zero and configuring \mathbf{R}_k as the identity matrix. All elements of the principal diagonal of \mathbf{H}_k are set to a uniform value to ensure well-conditioned components.

The users can manually configure other component parameters, such as location \mathbf{m}_k , minimum function value σ_k , and the matrix \mathbf{H}_k . This flexibility allows for the design of problem instances with specific deceptiveness characteristics. However, manual configuration can become cumbersome when dealing with a large number of components. To simplify this process, these parameters can be randomized within user-defined ranges, allowing users to focus primarily on varying the value of o . For a comprehensive analysis of the impact of multiple promising regions, we recommend varying the number of components o across a broad spectrum, for example, $o \in \{1, 2, 5, 10, 25, 50\}$.

F. Exploring Complex Combinations of Challenges and Features

Sections III-A through III-E elaborated on generating problem instances tailored to examine specific problem characteristics in isolation, ensuring that external factors do not unduly influence algorithmic performance. Such specialized testing capabilities are a distinctive offering of GNBG. Nevertheless, real-world scenarios frequently present a tapestry of intertwined challenges and characteristic combinations, leading to increased intricacies. Leveraging the inherent adaptability of GNBG, researchers can construct an expansive array of problem instances, each mirroring the multifaceted nature of real-world optimization problems. In the following, we outline a series of methodologies to craft problem instances that blend diverse problem characteristics and challenges, tailored to meet specific research objectives.

Diverse single-component problem instances, embodying multiple challenges, can be crafted by combining the configurations detailed in Sections III-A through III-D. For instance, by configuring the matrix \mathbf{H} as delineated in Section III-B and adjusting $\boldsymbol{\mu}$ and $\boldsymbol{\omega}$ based on the guidelines of Section III-D, researchers can synthesize problem landscapes that are both ill-conditioned and multimodal. This facilitates targeted investigations into algorithmic performance under specific complexities and characteristics. GNBG’s versatility enables the generation of numerous problem instances with various combinations of characteristics in a controllable manner. As an illustrative example, Figure 7(a) portrays a landscape containing an ill-conditioned, sub-linear, rotated, multimodal, and asymmetric component. To generate more complex problem instances, GNBG facilitates the construction of landscapes with multiple components, each exhibiting distinct characteristics and complexities. Figure 7(b) offers a visual representation of a problem instance housing two distinct components, each with unique parameter settings like size, shape, and rotation angle. This serves to spotlight GNBG’s prowess in crafting intricate landscapes bearing discrete attributes. Observably, while the narrower component encompasses the global optimum, its counterpart spans a more considerable expanse, with its basin of attraction enveloping a significant portion of the search space. Such landscapes are inherently deceptive.

A specific class of challenging optimization problems features landscapes where the optimal solution lies within a valley, such as the Rosenbrock function³. In these problems, after an algorithm converges to the valley’s base, it must

³Also known as the banana valley.

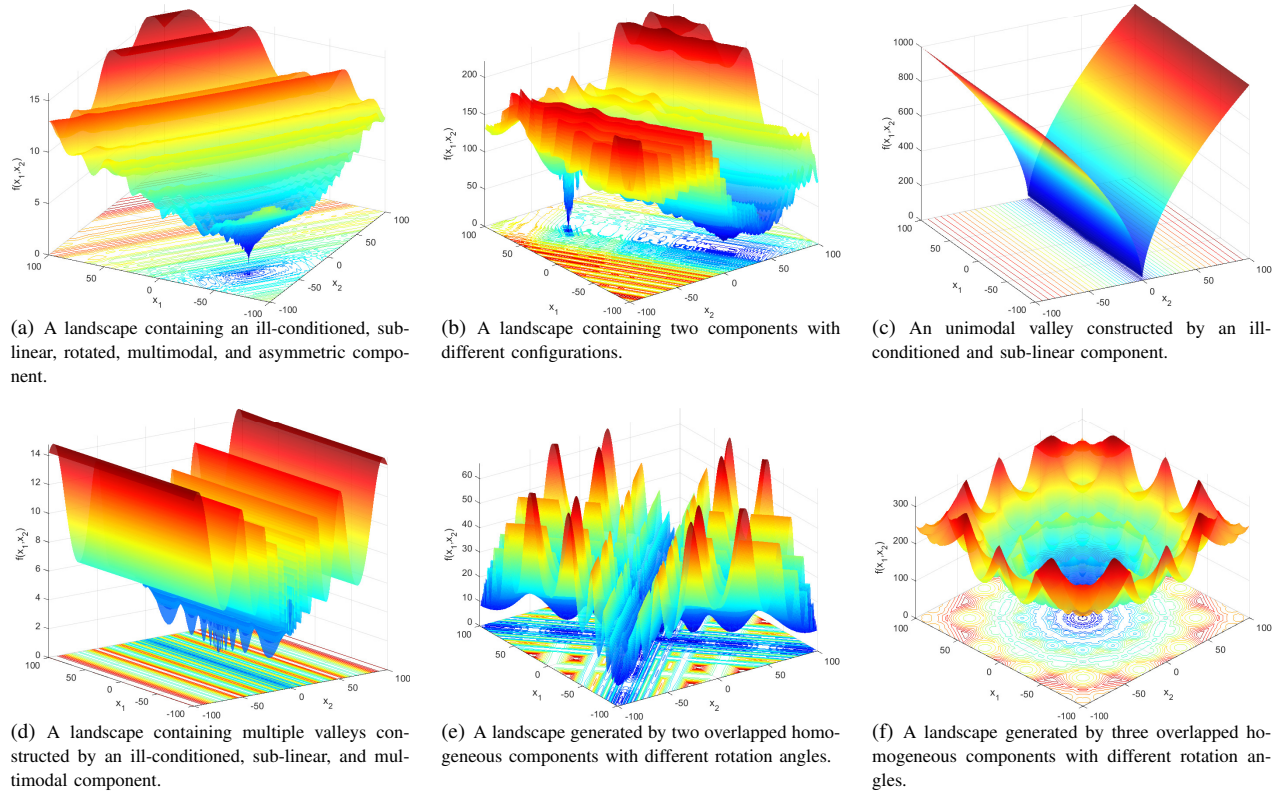


Fig. 7: Problem instances generated by GNBG with various combinations of characteristics and challenges.

navigate a specific path to find the optimal solution—a task that proves difficult for many algorithms. By incorporating sub-linear and highly ill-conditioned basins, we can create such valleys using GNBG. A higher degree of ill-conditioning in the matrix \mathbf{H} combined with lower λ values results in narrower valleys, typically making the problem more arduous. Figure 7(c) showcases an example of a unimodal problem instance with a pronounced narrow valley, as generated by GNBG. Employing the transformation \mathbb{T} can heighten the problem’s complexity substantially, leading to landscapes with multiple valleys, only one of which houses the global optimum. Intriguingly, this dominant valley may be interspersed with local minima, further complicating the task of navigating its irregular and rugged terrain to find the global optimum. Figure 7(d) illustrates such a multifaceted problem landscape. The challenge intensifies when these problems exhibit intricate variable interaction structures, further complicating the path-following process needed to locate the global optimum.

Figures 7(f) and 7(e) highlight another capability of GNBG when employing multiple components: the generation of a “hybrid component” by overlapping several components with identical minimum positions and values. In these depicted landscapes, two and three components are utilized, respectively. Though each component shares the same parameter settings in a given plot, they exhibit different rotation angles. This technique allows for the fusion of various components, culminating in a hybrid component endowed with unique morphological characteristics not achievable with a single component.

G. Delving into Scalability: Adjusting the Dimensionality of Problem Instances

One of the defining attributes of GNBG is its scalability. The problem instances it generates are inherently adjustable with respect to dimension d . Researchers have the flexibility to specify d based on their investigative goals. This adaptability is instrumental when probing the resilience of optimization algorithms, especially as the dimensionality increases. Such scalability becomes especially pertinent when examining algorithmic behaviors in the presence of challenges like ill-conditioning, multimodality, and intricate variable interaction structures. GNBG offers the versatility to produce problem instances across a wide range of dimensions, facilitating experiments with, for instance, dimensions set as $d \in \{10, 20, 30\}$ or even broader spectrums.

IV. IMPACT OF VARIOUS DEGREES OF GNBG'S CONTROLLABLE CHARACTERISTICS ON THE PERFORMANCE OF ALGORITHMS

In this section, we present a preliminary investigation into the impact of various degrees of problem characteristics generated by GNBG on the performance of three well-known optimization algorithms:

- Pattern Search (PS) [45]: A direct search method and an exemplar of single-solution-based techniques.
- Particle Swarm Optimization (PSO) [46, 47]: A paradigmatic swarm intelligence algorithm and a population-based method.
- Differential Evolution (DE) [48, 49]: An archetypal evolutionary algorithm, also population-based.

We employed the generalized PS with adaptive mesh and orthogonal polling directions [50, 51] in the experiments. We configured PSO with a constriction factor and global star neighborhood topology, setting $c_1 = c_2 = 2.05$ and $\chi = 0.729843788$ [52]. For DE, the strategy adopted is *DE/rand/1/bin* with F and Cr values of 0.9 and 0.5, respectively [49]. The population size is set to 100 for both PSO and DE.

Our experimental methodology involves repeating each test 31 times, employing distinct random seeds for the algorithms in each run. Each experiment is designed to examine the effects of varying a specific GNBG parameter. This variation allows us to observe algorithmic performance as they address varying intensities of a particular problem characteristic. Results, in terms of both mean and standard deviation, are collated in Tables II to VII. In Tables II to VII, we provide the mean absolute error (and standard deviation in the parenthesis) of the best-found solution at function evaluation milestones: 100,000, 250,000, and 500,000. Moreover, with an acceptance threshold set at 10^{-8} , we provide the mean number of required function evaluations to find a solution within this error bound [5, 23]. Any run reaching this threshold is labeled successful, and we subsequently report the success rate over the 31 iterations.

Note that the experiments conducted in this section aim to gain preliminary insights into the impact of different degrees of problem characteristics on the performance of the aforementioned optimization algorithms. While we aim to provide initial findings in this section, conducting a comprehensive empirical study, involving a wider array of algorithms and problem instances, is beyond the scope of this paper and is a potential avenue for future work. However, this preliminary investigation lays the foundation for future research in exploring the performance of other algorithms with GNBG-generated problem characteristics.

In Table II, we delve into the influence of basin linearity variations on the performance of algorithms. Adjusting the parameter λ allows for modulation of the basin's linearity for each component, spanning from highly sub-linear to linear, and on to highly super-linear. Our focus for the experiments outlined in this table is solely on unimodal problem instances, offering a targeted investigation into the ramifications of basin linearity (see Section III-A). The results presented underscores the increased difficulty in exploiting problem instances characterized by smaller λ values. This observation is corroborated by the evident increase in function evaluations needed to meet the acceptance threshold as λ decreases. Moreover, assessing the results at distinct function evaluation checkpoints reveals a discernible deterioration in performance for PSO and DE when tackling instances with reduced λ values. This suggests that components typified by sub-linear basins of attraction pose a greater challenge compared to their linear and super-linear counterparts.

One notable observation from the table is the rapid convergence speeds exhibited by PS and PSO. Although their convergence speeds are influenced by heightened degrees of sub-linearity (specifically, smaller λ values), they invariably attain the designated acceptance threshold. In contrast, DE's performance is sensitive to escalating sub-linearity degrees. Notably, when λ is pegged at 0.1, DE struggles to locate an acceptable solution even after 500,000 function evaluations.

The next controllable attribute for each component is its conditioning. This can be modulated by specifying distinct values to the principal diagonal elements of the matrix \mathbf{H} . Table III elucidates the effects of diverse condition numbers, leading to varying ill-conditioning magnitudes, on the performance of algorithms. The experiments encapsulated in this table cater exclusively to unimodal problem instances, thus allowing a dedicated exploration into the implications of conditioning (see Section III-B). A conspicuous trend from the results is the escalating challenge posed to the algorithms as the condition number of problem instances amplifies. This is evident by the notable rise in function evaluations required to attain the acceptance threshold with an increase in the condition number. Furthermore, a meticulous assessment of outcomes at the specified function evaluation junctures indicates a tangible decline in PSO and DE performance when confronted with elevated condition numbers. Another observation is that, PSO, in certain runs, exhibits stagnation issues when the condition number surges to 10^5 or beyond.

The structure of variable interactions stands as an important aspect of optimization problems, significantly influencing the performance of algorithms. Table IV shows the results obtained by the algorithms on problem instances with various variable interaction structures: from fully separable (where $p = 0$) to fully connected non-separable configurations (where $p = 1$). Using the GNBG parameter settings outlined in Section III-C, we generated instances specifically designed to evaluate the impact of various degrees of connectivity in variable interaction structures on algorithm performance. As the value of p escalates, the intricacy of the variable interaction structure amplifies, thereby exerting a considerable impact on the performance of algorithms. Notably, while the convergence rates of PS and DE deteriorate in solving instances

TABLE II: Impact of various values of λ on the performance of algorithms. For the remaining GNBG parameters, we set $o = 1$, $d = 30$, $\mathbf{m} = \{m_i = 0 \mid i = 1, 2, \dots, d\}$, $\sigma = 0$, $\boldsymbol{\mu} = (0, 0)$, $\boldsymbol{\omega} = (0, 0, 0, 0)$, $\mathbf{R}_{d \times d} = \mathbf{H} = \mathbf{I}_{d \times d}$, and the search space is bounded to $[-100, 100]$.

Algorithm	λ	Average of absolute error at			Average FE to success	Success rate
		100,000 FE	250,000 FE	500,000 FE		
PS	0.10	0(0)	0(0)	0(0)	72382.12(1903.93)	100
	0.25	0(0)	0(0)	0(0)	72533.03(1780.78)	100
	0.50	0(0)	0(0)	0(0)	48158.00(1246.49)	100
	0.75	0(0)	0(0)	0(0)	35463.09(1255.63)	100
	1.00	0(0)	0(0)	0(0)	29062.74(1003.90)	100
PSO	0.10	0.0069(0.0011)	8.43e-07(1.90e-07)	2.59e-13(9.45e-14)	323428.09(5423.11)	100
	0.25	4.25e-06(2.12e-06)	7.08e-16(5.64e-16)	4.34e-32(4.1896e-32)	140119.51(3766.76)	100
	0.50	2.17e-11(1.60e-11)	7.47e-31(1.07e-30)	3.70e-63(1.1108e-62)	78339.70(2503.35)	100
	0.75	1.07e-16(2.03e-16)	7.59e-46(2.49e-45)	5.26e-94(1.5645e-93)	57584.54(2701.37)	100
	1.00	2.34e-22(4.52e-22)	2.62e-61(5.55e-61)	3.25e-126(8.80e-126)	46538.09(1617.94)	100
DE	0.10	0.1788(0.0107)	0.0028(0.0003)	2.96e-06(3.63e-07)	–	0
	0.25	0.0134(0.0021)	4.40e-07(8.22e-08)	1.51e-14(5.13e-15)	304393.06(2973.64)	100
	0.50	0.0002(5.29e-05)	2.06e-13(1.02e-13)	2.66e-28(1.60e-28)	171144.48(2426.48)	100
	0.75	3.24e-06(1.96e-06)	1.24e-19(1.04e-19)	4.67e-42(5.19e-42)	127166.41(3162.47)	100
	1.00	4.59e-08(2.81e-08)	6.89e-26(8.38e-26)	1.23e-55(2.39e-55)	104753.80(2409.21)	100

TABLE III: Impact of various conditioning (represented by the condition number of \mathbf{H}) on the performance of optimization algorithms. The fixed GNBG parameters are: $o = 1$, $d = 30$, $\mathbf{m} = \{m_i = 0 \mid i = 1, 2, \dots, d\}$, $\sigma = 0$, $\lambda = 1$, $\boldsymbol{\mu} = (0, 0)$, $\boldsymbol{\omega} = (0, 0, 0, 0)$, and $\mathbf{R}_{d \times d} = \mathbf{I}_{d \times d}$ with search space constrained to $[-100, 100]$. For the Beta distribution, which randomizes the principal diagonal of \mathbf{H} , both α and β are set to 0.4. Notably, a consistent random seed is applied to the Beta distribution across all runs.

Algorithm	Condition#	Average of absolute error at			Average FE to success	Success rate
		100,000 FE	250,000 FE	500,000 FE		
PS	1	0(0)	0(0)	0(0)	29062.74(1003.90)	100
	10	0(0)	0(0)	0(0)	31262.38(1226.66)	100
	10^2	0(0)	0(0)	0(0)	33226.45(1248.04)	100
	10^3	0(0)	0(0)	0(0)	35694.80(1198.01)	100
	10^4	0(0)	0(0)	0(0)	37590.77(1392.36)	100
	10^5	0(0)	0(0)	0(0)	40329.41(1221.96)	100
	10^6	0(0)	0(0)	0(0)	42726.35(1244.90)	100
	10^7	0(0)	0(0)	0(0)	45317.61(1382.11)	100
PSO	1	2.34e-22(4.52e-22)	2.62e-61(5.55e-61)	3.25e-126(8.80e-126)	46538.09(1617.94)	100
	10	1.42e-21(2.25e-21)	1.28e-59(3.20e-59)	7.36e-124(3.21e-123)	49473.61(1548.64)	100
	10^2	2.91e-18(1.38e-17)	1.06e-56(5.57e-56)	1.20e-122(5.18e-122)	55086.16(3907.14)	100
	10^3	7.25e-16(4.02e-15)	3.42e-57(1.03e-56)	2.83e-122(7.39e-122)	59079.80(4484.42)	100
	10^4	6.87e-17(2.52e-16)	1.16e-55(4.22e-55)	7.91e-120(3.80e-11)	63156.87(3645.66)	100
	10^5	322.5806(1796.0530)	322.5806(1796.0530)	322.5806(1796.0530)	67873.96(3505.80)	96.77
	10^6	645.1613(2497.3104)	645.1613(2497.3104)	645.1613(2497.3104)	72797.48(5149.41)	93.54
	10^7	322.5806(1796.0530)	322.5806(1796.0530)	322.5806(1796.053)	77139.33(6396.48)	96.7742
DE	1	4.59e-08(2.81e-08)	6.89e-26(8.38e-26)	1.23e-55(2.39e-55)	104753.80(2409.21)	100
	10	1.56e-07(1.37e-07)	2.50e-25(3.87e-25)	3.34e-55(4.84e-55)	109257.19(2219.66)	100
	10^2	1.29e-06(8.49e-07)	2.26e-24(2.48e-24)	2.60e-54(4.48e-54)	117002.19(2287.84)	100
	10^3	9.78e-06(5.60e-06)	1.20e-23(1.37e-23)	2.06e-53(3.06e-53)	124048.58(2728.30)	100
	10^4	0.0001(7.21e-05)	1.30e-22(1.21e-22)	3.16e-52(3.70e-52)	133027.70(2543.55)	100
	10^5	0.0009(0.0005)	1.1e-21(1.08e-21)	1.49e-51(1.63e-51)	140942.16(2467.07)	100
	10^6	0.0070(0.0046)	1.13e-20(1.76e-20)	1.24e-50(1.51e-50)	148441.58(2736.83)	100
	10^7	0.0601(0.0286)	7.67e-20(9.44e-20)	1.28e-49(2.06e-49)	156012.54(2733.30)	100

with more complex variable interaction structures, they nonetheless ascertain acceptable solutions—albeit at the expense of increased function evaluations. Conversely, PSO struggles with heightened complexity in variable interaction structures. This is manifested in its occasional stagnation or markedly sluggish convergence rate, inhibiting it from finding an acceptable solution within a budget of 500,000 function evaluations. Furthermore, it is discernible that the success rate of PSO wanes with the intensifying complexity of the variable interaction structure, a consequence of augmenting p values.

In our experiments evaluating the impact of variable interaction structures, we employ randomized angles for each connection in Θ . These angles dictate the strength of the connections between variables. Table V presents the influence of three specific angles—0, $\frac{5\pi}{180}$, and $\frac{\pi}{4}$ —on the performance of algorithms. Adhering to the GNBG parameter settings delineated in Section III-C, we set $p = 1$, meaning all elements above the principal diagonal of Θ assume the designated angle. Unsurprisingly, the best results emerge when the angle is zero, preserving the component's original variable interaction

TABLE IV: Performance impact of varying p values, dictating degrees of variable interaction structure connectivity, on optimization algorithms. Fixed GNBG parameters include: $o = 1$, $d = 30$, $\mathbf{m} = \{m_i = 0 \mid i = 1, 2, \dots, d\}$, $\sigma = 0$, $\lambda = 1$, $\boldsymbol{\mu} = (0, 0)$, and $\boldsymbol{\omega} = (0, 0, 0, 0)$, with the search space bound to $[-100, 100]$. The principal diagonal of \mathbf{H} is randomized using a uniform distribution in $[1, 100]$ to induce moderate ill-conditioning and make component rotation dependent. A consistent random seed is applied for both \mathbf{H} and p randomizations across runs.

Algorithm	p	Absolute error at			Average FE to success	Success rate
		100,000 FE	250,000 FE	500,000 FE		
PS	0.00	0(0)	0(0)	0(0)	33405.09(1061.08)	100
	0.25	0.057616(0.0829)	1.63e-10(3.71e-10)	1.81e-24(7.72e-24)	203970.61(22421.50)	100
	0.50	0.011233(0.0157)	1.50e-12(1.92e-12)	6.81e-29(1.64e-28)	186118.77(10970.198)	100
	0.75	0.037089(0.0354)	4.52e-11(6.40e-11)	2.84e-26(4.44e-26)	203580.54(15404.26)	100
	1.00	0.090223(0.1733)	5.85e-10(1.01e-09)	1.08e-23(2.86e-23)	213361.41(21342.67)	100
PSO	0.00	2.3459e-18(1.2246e-17)	7.1694e-58(2.5105e-57)	1.9225e-123(8.4677e-123)	55584.16(3610.69)	100
	0.25	9.0549(11.9187)	0.0050(0.0062)	7.8924e-07(1.5512e-06)	454501.70(35548.89)	32.25
	0.50	25.4761(28.5542)	0.0611(0.1141)	1.2766e-05(2.1924e-05)	458912.37(38169.85)	22.58
	0.75	22.5156(20.0315)	0.0571(0.1871)	5.1357e-06(3.7560e-05)	458343.00(34410.20)	12.90
	1.00	17.1599(18.5575)	0.0174(0.0237)	9.2786e-06(2.2028e-05)	490021.50(11434.62)	6.45
DE	0.00	1.38e-06(8.69e-07)	1.91e-24(1.74e-24)	3.99e-54(7.02e-54)	117446.22(2673.65)	100
	0.25	0.8026(0.9358)	1.13e-07(3.78e-07)	3.84e-19(1.99e-18)	247990.00(23662.44)	100
	0.50	1.5307(1.9609)	6.36e-08(8.41e-08)	3.07e-19(1.42e-18)	258567.16(17237.18)	100
	0.75	0.6017(0.9387)	2.75e-09(4.07e-09)	1.19e-22(2.1e-22)	234734.48(10813.28)	100
	1.00	0.8036(0.7247)	3.92e-08(7.48e-08)	1.35e-20(4.28e-20)	250733.80(15214.93)	100

TABLE V: Impact of various angles on the performance of algorithms. The angles determine interaction strength within a fully-connected variable interaction structure. the remaining GNBG settings are: $o = 1$, $d = 30$, $\mathbf{m} = \{m_i = 0 \mid i = 1, 2, \dots, d\}$, $\sigma = 0$, $\lambda = 1$, $\boldsymbol{\mu} = (0, 0)$, $\boldsymbol{\omega} = (0, 0, 0, 0)$ with search boundaries $[-100, 100]$. The uniform distribution randomizes \mathbf{H} 's diagonal within $[1, 100]$ to introduce moderate ill-conditioning and dependency in component rotation. A consistent random seed is applied for \mathbf{H} randomizations across runs.

Algorithm	Angle	Absolute error at			Average FE to success	Success rate
		100,000 FE	250,000 FE	500,000 FE		
PS	0	0(0)	0(0)	0(0)	33405.09(1061.08)	100
	$5 \frac{\pi}{180}$	0.0001(0.0001)	2.87e-17(1.21e-16)	3.51e-39(1.70e-38)	140831.58(10479.61)	100
	$\frac{\pi}{4}$	0.0867(0.0944)	1.46e-10(1.73e-10)	1.09e-24(1.80e-24)	211963.00(12301.48)	100
PSO	0	2.34e-18(1.22e-17)	7.16e-58(2.51e-57)	1.92e-123(8.46e-123)	55584.1613(3610.69)	100
	$5 \frac{\pi}{180}$	1777.687(9896.2039)	0.0054(0.0304)	2.20e-11(1.189e-10)	309116.29(44254.11)	100
	$\frac{\pi}{4}$	44.8274(49.1275)	0.1231(0.1691)	5.63e-05(8.07e-05)	-	0
DE	0	1.38e-06(8.69e-07)	1.91e-24(1.74e-24)	3.99e-54(7.02e-54)	117446.22(2673.65)	100
	$5 \frac{\pi}{180}$	0.0463(0.0783)	9.25e-12(3.06e-11)	3.26e-28(1.28e-27)	192322.38(9867.75)	100
	$\frac{\pi}{4}$	2.7704(2.9605)	1.61e-06(3.72e-06)	4.30e-17(1.31e-16)	281307.45(18729.14)	100

and yielding a fully separable structure. Assigning angles of $\frac{5\pi}{180}$ and $\frac{\pi}{4}$ transforms the component's interaction structure into a non-separable, fully-connected state, increasing the problem's complexity. The degree of this increase, however, is contingent upon the strength of variable interactions. Based on the results, the problem is easier to tackle when the angle is set to $\frac{5\pi}{180}$ compared to $\frac{\pi}{4}$. This suggests that components become easier to exploit as angles approach axes-aligned values (i.e., angles close to $k\frac{\pi}{2}$ where $k \in \mathbb{Z}$).

In prior experiments, we employed unimodal components by setting all elements of $\boldsymbol{\mu}$ and $\boldsymbol{\omega}$ to zero. This effectively neutralized the \mathbb{T} transformation. Table VI delves into the effects of varying $\boldsymbol{\mu}$ and $\boldsymbol{\omega}$ on algorithmic performance, with GNBG parameter adjustments described in Section III-D.

The analysis indicates that better results are obtained when both $\boldsymbol{\mu}$ and $\boldsymbol{\omega}$ are set to smaller values, which correspond to fewer and shallower local optima. In addition, higher $\boldsymbol{\mu}$ values manifest more arduous instances, marked by pronounced local optima depths. Such depths augment the risk of premature convergence: deeper local optima necessitate extended convergence periods, during which algorithms might diminish their diversity, leading to potential entrapment within local optima. A pivotal observation reveals that, with larger $\boldsymbol{\mu}$ values, components with elevated $\boldsymbol{\omega}$ values prove more problematic than their counterparts with lower $\boldsymbol{\omega}$ values. For instance, when $\boldsymbol{\mu}$ is $[0.25, 0.25]$, an increment in $\boldsymbol{\omega}$ from 5 to 50 impairs the exploration capabilities of DE and PS, causing them to become ensnared in local optima. This behavior can be attributed to greater $\boldsymbol{\omega}$ values spawning an increased count of local optima, amplifying problem ruggedness. Additionally, the results highlight that all tested algorithms are prone to local optima confinement with $\boldsymbol{\mu}$ values of 0.5 or above. It is noteworthy that, upon escalating the $\boldsymbol{\mu}$ values, while algorithms may yield improved average absolute error values, such enhancements are driven by the depth of local optima and the consequential reduction in function values at their bottoms.

TABLE VI: Impact of various values of μ and ω on the performance of algorithms. For the remaining GNBG parameters, we set $o = 1$, $d = 30$, $\mathbf{m} = \{m_i = 0 \mid i = 1, 2, \dots, d\}$, $\sigma = 0$, $\boldsymbol{\mu} = (0, 0)$, $\lambda = 1$, $\mathbf{R}_{d \times d} = \mathbf{H} = \mathbf{I}_{d \times d}$, and the search space is bounded to $[-100, 100]$.

Algorithm	μ	ω	Absolute error at			Average FE to success	Success rate
			100,000 FE	250,000 FE	500,000 FE		
PS	[0.00,0.00]	[0,0,0,0]	0(0)	0(0)	0(0)	29062.74(1003.90)	100
	[0.10,0.10]	[5,5,5,5]	0(0)	0(0)	0(0)	29305(1123.002)	100
	[0.25,0.25]	[5,5,5,5]	0(0)	0(0)	0(0)	29609.5161(980.6566)	100
	[0.50,0.50]	[5,5,5,5]	18.0895(12.3199)	18.0895(12.3199)	18.0895(12.3199)	–	0
	[0.75,0.75]	[5,5,5,5]	95.264(60.0162)	95.264(60.0162)	95.264(60.0162)	–	0
	[1.00,1.00]	[5,5,5,5]	558.9562(406.1115)	558.9562(406.1115)	558.9562(406.1115)	–	0
	[0.10,0.10]	[50,50,50,50]	0(0)	0(0)	0(0)	29208.6774(1051.6833)	100
	[0.25,0.25]	[50,50,50,50]	0(0)	0(0)	0(0)	29404.5806(940.7578)	100
	[0.50,0.50]	[50,50,50,50]	647.9814(632.4114)	647.9814(632.4114)	647.9814(632.4114)	–	0
	[0.75,0.75]	[50,50,50,50]	638.8819(395.0779)	638.8819(395.0779)	638.8819(395.0779)	–	0
[1.00,1.00]	[50,50,50,50]	444.1268(220.0597)	444.1268(220.0597)	444.1268(220.0597)	–	0	
PSO	[0.00,0.00]	[0,0,0,0]	2.34e-22(4.52e-22)	2.62e-61(5.55e-61)	3.25e-126(8.80e-126)	46538.09(1617.94)	100
	[0.10,0.10]	[5,5,5,5]	1.77e-18(5.10e-18)	8.96e-51(4.95e-50)	1.27e-108(6.00e-108)	53903.74(3078.32)	100
	[0.25,0.25]	[5,5,5,5]	4035.4152(3934.659)	4035.4152(3934.659)	4035.4152(3934.659)	–	0
	[0.50,0.50]	[5,5,5,5]	11898.8015(5539.7218)	11898.8015(5539.7218)	11898.8015(5539.7218)	–	0
	[0.75,0.75]	[5,5,5,5]	7893.1048(2127.2207)	7889.9318(2130.3158)	7889.9318(2130.3158)	–	0
	[1.00,1.00]	[5,5,5,5]	3779.0472(1189.2953)	3754.5283(1169.8409)	3744.1726(1172.5886)	–	0
	[0.10,0.10]	[50,50,50,50]	15.7274(47.7612)	15.7274(47.7612)	15.7274(47.7612)	57410.625(3422.444)	51.6129
	[0.25,0.25]	[50,50,50,50]	415.5687(980.777)	415.5687(980.777)	415.5687(980.777)	–	0
	[0.50,0.50]	[50,50,50,50]	4895.7732(3780.7165)	4701.8173(3589.9746)	4701.8094(3589.9644)	–	0
	[0.75,0.75]	[50,50,50,50]	5820.2932(2246.9847)	4876.6711(2224.7195)	4815.8523(2259.8326)	–	0
[1.00,1.00]	[50,50,50,50]	2749.6023(1014.685)	2435.603(956.475)	2291.4915(1003.7711)	–	0	
DE	[0.00,0.00]	[0,0,0,0]	4.59e-08(2.81e-08)	6.89e-26(8.38e-26)	1.23e-55(2.39e-55)	104753.80(2409.21)	100
	[0.10,0.10]	[5,5,5,5]	2.2493e-07(1.4234e-07)	3.5348e-24(3.2999e-24)	4.4086e-52(6.6203e-52)	110902.1613(2229.8682)	100
	[0.25,0.25]	[5,5,5,5]	0.0012916(0.00067359)	1.1893e-14(1.4515e-14)	6.4408e-33(1.3301e-32)	166925.7742(5081.816)	100
	[0.50,0.50]	[5,5,5,5]	880.0988(453.4637)	14.5252(12.9632)	0.032015(0.035991)	–	0
	[0.75,0.75]	[5,5,5,5]	2887.0515(581.4986)	1406.0535(433.1411)	322.9837(148.5842)	–	0
	[1.00,1.00]	[5,5,5,5]	4716.9576(1387.7579)	2134.4184(627.5284)	619.71(207.0421)	–	0
	[0.10,0.10]	[50,50,50,50]	2.8002e-07(1.6446e-07)	9.3976e-24(7.7403e-24)	3.5197e-51(5.6973e-51)	112765.9355(2191.2871)	100
	[0.25,0.25]	[50,50,50,50]	0.0015645(0.001421)	9.6231e-15(7.3691e-15)	2.7353e-33(3.2895e-33)	167646.6129(3837.7284)	100
	[0.50,0.50]	[50,50,50,50]	177.2765(86.7903)	0.19943(0.22682)	2.7076e-06(7.8304e-06)	–	0
	[0.75,0.75]	[50,50,50,50]	5587.9928(1846.9089)	2000.9528(880.6734)	472.9545(359.5097)	–	0
[1.00,1.00]	[50,50,50,50]	11919.8398(3413.1434)	6632.5713(2143.617)	3237.6569(1430.2877)	–	0	

Finally, Table VII showcases the influence of the number of components in the landscape on algorithm performance. The GNBG parameter configurations for these tests are detailed in Section III-E. Due to the presence of multiple promising regions, each with a substantial basin of attraction, these problems can prove exceptionally deceptive. A deceptive search space arises when extensive, low-function-value regions⁴ mislead optimization algorithms, making them appear more favorable than they truly are. In such situations, algorithms might become ensnared in these deceptive basins, inhibiting them from discovering the global optimum. Results suggest that the presence of multiple components profoundly impacts algorithmic efficiency. Interestingly, when o is set to two, the success rates diminish considerably. Our analyses reveal that based on the constant random seed employed for generating this instance, the component containing the global optimum occupies a smaller portion of the landscape than its counterpart. Under this deceptive guise, algorithms predominantly gravitate toward the larger, yet misleading, promising region. Data from instances with a greater number of promising regions indicate that algorithms rapidly converge to a deceptive region and become trapped therein. It is paramount to note that the average absolute error values in these scenarios are not only dictated by the component count but depend on the level of deception and the quality of the dominant deceptive components. Nonetheless, it is evident that algorithms struggle to pinpoint the global optimum when component numbers exceed two.

V. CONCLUSION

This paper introduced the Generalized Numerical Benchmark Generator (GNBG), an innovative tool for generating problem instances with a diverse range of controllable characteristics. Harnessing the power of a unique parametric baseline function, GNBG offers researchers control over attributes like dimensionality, variable interaction structures, conditioning, basin morphology, multimodality, ruggedness, symmetry, and deceptiveness.

Through a preliminary investigation, we examined the influence of these attributes on the performance of multiple optimization algorithms. This exploration illuminated the strengths and weaknesses of these algorithms when navigating complexities caused by different degrees of problem characteristics. Our results highlight the significant impact of GNBG's

⁴In minimization problems, low-function-values signify values of superior quality.

TABLE VII: Assessing the performance impact of varying component numbers on optimization algorithms. For each component k , parameters are set as $d = 30$, $\mu_k = (0, 0)$, $\lambda_k = 1$, and $\mathbf{R}_k = \mathbf{I}_{d \times d}$ with search boundaries $[-100, 100]$. The minimum position (\mathbf{m}_k) and value (σ_k) for each component k are randomly designated within $[-100, 100]$ and $[0, 10]$, respectively. Furthermore, all elements on the principal diagonal of \mathbf{H}_k are uniformly randomized within $[0.001, 0.1]$ (all have the same value), signifying varied sizes among components while ensuring they remain well-conditioned. Consistent random seeds are used across runs for GNBG instance generation.

Algorithm	σ	Absolute error at			Average FE to success	Success rate
		100,000 FE	250,000 FE	500,000 FE		
PS	1	0(0)	0(0)	0(0)	29062.74(1003.90)	100
	2	8.2578(2.2045)	8.2578(2.2045)	8.2578(2.2045)	30194(2049.1955)	6.4516
	5	44.7651(1.7597e-14)	44.7651(1.7597e-14)	44.7651(1.7597e-14)	–	0
	10	12.8672(7.2125)	12.8672(7.2125)	12.8672(7.2125)	–	0
	25	19.03(0.48748)	19.03(0.48748)	19.03(0.48748)	–	0
	50	17.358(14.8416)	17.358(14.8416)	17.358(14.8416)	–	0
PSO	1	2.34e-22(4.52e-22)	2.62e-61(5.55e-61)	3.25e-126(8.80e-126)	46538.09(1617.94)	100
	2	7.4035(3.3003)	7.4035(3.3003)	7.4035(3.3003)	52109(5809.1577)	16.129
	5	99.7869(306.3483)	99.7869(306.3483)	99.7869(306.3483)	–	0
	10	13.7992(6.8719)	13.7992(6.8719)	13.7992(6.8719)	–	0
	25	43.5034(136.2469)	43.5034(136.2469)	43.5034(136.2469)	–	0
	50	20.5219(14.7587)	20.5219(14.7587)	20.5219(14.7587)	–	0
DE	1	4.59e-08(2.81e-08)	6.89e-26(8.38e-26)	1.23e-55(2.39e-55)	104753.80(2409.21)	100
	2	8.5426(1.5854)	8.5426(1.5854)	8.5426(1.5854)	114346(0)	3.2258
	5	44.7651(4.47e-08)	44.7651(1.44e-14)	44.7651(1.44e-14)	–	0
	10	17.111(2.03e-08)	17.111(1.08e-14)	17.111(1.08e-14)	–	0
	25	18.9424(2.01e-08)	18.9424(3.61e-15)	18.9424(3.61e-15)	–	0
	50	12.997(15.3686)	12.997(15.3686)	12.997(15.3686)	–	0

adjustable characteristics on algorithmic performance. Elements such as intricate variable interaction structures and specific attributes of local optima, including their depth and width, posed differential challenges to the algorithms under scrutiny. While our insights are enlightening, they are, by nature, preliminary, indicating a clear demand for broader and more in-depth studies. As a future work, a comprehensive empirical study focusing on a wide array of optimization algorithms and GNBG-generated problem instances will be of paramount importance.

REFERENCES

- [1] M. Cousineau, V. Verter, S. A. Murphy, and J. Pineau, “Estimating causal effects with optimization-based methods: A review and empirical comparison,” *European Journal of Operational Research*, vol. 304, no. 2, pp. 367–380, 2023.
- [2] S. S. Rao, *Engineering optimization: theory and practice*. John Wiley & Sons, 2019.
- [3] C. Archetti, L. Peirano, and M. G. Speranza, “Optimization in multimodal freight transportation problems: A survey,” *European Journal of Operational Research*, vol. 299, no. 1, pp. 1–20, 2022.
- [4] V. Beiranvand, W. Hare, and Y. Lucet, “Best practices for comparing optimization algorithms,” *Optimization and Engineering*, vol. 18, pp. 815–848, 2017.
- [5] T. Bartz-Beielstein, C. Doerr, D. v. d. Berg, J. Bossek, S. Chandrasekaran, T. Eftimov, A. Fischbach, P. Kerschke, W. La Cava, M. Lopez-Ibanez *et al.*, “Benchmarking in optimization: Best practice and open issues,” *arXiv preprint arXiv:2007.03488*, 2020.
- [6] N. Hansen, S. Finck, R. Ros, and A. Auger, “Real-parameter black-box optimization benchmarking 2009: Noiseless functions definitions,” Tech. Rep., 2009.
- [7] D. Whitley, J.-P. Watson, A. Howe, and L. Barbulescu, “Testing, evaluation and performance of optimization and learning systems,” in *Adaptive Computing in Design and Manufacture V*. Springer, 2002, pp. 27–39.
- [8] O. M. Shir, C. Doerr, and T. Bäck, “Compiling a benchmarking test-suite for combinatorial black-box optimization: a position paper,” in *Proceedings of the Genetic and Evolutionary Computation Conference Companion*, 2018, pp. 1753–1760.
- [9] K. M. Malan and A. P. Engelbrecht, “A survey of techniques for characterising fitness landscapes and some possible ways forward,” *Information Sciences*, vol. 241, pp. 148–163, 2013.
- [10] M. A. Muñoz, Y. Sun, M. Kirley, and S. K. Halgamuge, “Algorithm selection for black-box continuous optimization problems: A survey on methods and challenges,” *Information Sciences*, vol. 317, pp. 224–245, 2015.
- [11] M. A. Muñoz and K. Smith-Miles, “Generating new space-filling test instances for continuous black-box optimization,” *Evolutionary computation*, vol. 28, no. 3, pp. 379–404, 2020.
- [12] E. Uchoa, D. Pecin, A. Pessoa, M. Poggi, T. Vidal, and A. Subramanian, “New benchmark instances for the capacitated vehicle routing problem,” *European Journal of Operational Research*, vol. 257, no. 3, pp. 845–858, 2017.

- [13] P. Kerschke and H. Trautmann, “Comprehensive feature-based landscape analysis of continuous and constrained optimization problems using the r-package flacco,” *Applications in Statistical Computing: From Music Data Analysis to Industrial Quality Improvement*, pp. 93–123, 2019.
- [14] A. H. Gandomi and X.-S. Yang, “Evolutionary boundary constraint handling scheme,” *Neural Computing and Applications*, vol. 21, pp. 1449–1462, 2012.
- [15] S. Helwig, J. Branke, and S. Mostaghim, “Experimental analysis of bound handling techniques in particle swarm optimization,” *IEEE Transactions on Evolutionary Computation*, vol. 17, no. 2, pp. 259–271, 2012.
- [16] M. Arif, J. Chen, G. Wang, and H. T. Rauf, “Cognitive population initialization for swarm intelligence and evolutionary computing,” *Journal of Ambient Intelligence and Humanized Computing*, pp. 1–14, 2021.
- [17] J. Skålnes, M. B. Ahmed, L. M. Hvattum, and M. Stålhane, “New benchmark instances for the inventory routing problem,” *European Journal of Operational Research*, in press, 2023.
- [18] M. N. Omidvar, X. Li, and K. Tang, “Designing benchmark problems for large-scale continuous optimization,” *Information Sciences*, vol. 316, pp. 419–436, 2015.
- [19] R. S. Olson, W. La Cava, P. Orzechowski, R. J. Urbanowicz, and J. H. Moore, “Pmlb: a large benchmark suite for machine learning evaluation and comparison,” *BioData mining*, vol. 10, pp. 1–13, 2017.
- [20] K. Deb, L. Thiele, M. Laumanns, and E. Zitzler, “Scalable multi-objective optimization test problems,” in *Proceedings of the 2002 Congress on Evolutionary Computation. CEC’02 (Cat. No. 02TH8600)*, vol. 1. IEEE, 2002, pp. 825–830.
- [21] D. Yazdani, M. N. Omidvar, R. Cheng, J. Branke, T. T. Nguyen, and X. Yao, “Benchmarking continuous dynamic optimization: Survey and generalized test suite,” *IEEE Transactions on Cybernetics*, vol. 52, no. 5, pp. 3380–3393, 2022.
- [22] M. Hellwig and H.-G. Beyer, “Benchmarking evolutionary algorithms for single objective real-valued constrained optimization—a critical review,” *Swarm and evolutionary computation*, vol. 44, pp. 927–944, 2019.
- [23] N. Hansen, A. Auger, R. Ros, O. Mersmann, T. Tušar, and D. Brockhoff, “COCO: A platform for comparing continuous optimizers in a black-box setting,” *Optimization Methods and Software*, vol. 36, no. 1, pp. 114–144, 2021.
- [24] L. Mei and Q. Wang, “Structural optimization in civil engineering: a literature review,” *Buildings*, vol. 11, no. 2, p. 66, 2021.
- [25] D. Yazdani, R. Cheng, D. Yazdani, J. Branke, Y. Jin, and X. Yao, “A survey of evolutionary continuous dynamic optimization over two decades – part A,” *IEEE Transactions on Evolutionary Computation*, vol. 25, no. 4, pp. 609–629, 2021.
- [26] —, “A survey of evolutionary continuous dynamic optimization over two decades – part B,” *IEEE Transactions on Evolutionary Computation*, vol. 25, no. 4, pp. 630–650, 2021.
- [27] A. O. Kusakci and M. Can, “Constrained optimization with evolutionary algorithms: a comprehensive review,” *Southeast Europe journal of soft computing*, vol. 1, no. 2, 2012.
- [28] M. N. Omidvar, X. Li, and X. Yao, “A review of population-based metaheuristics for large-scale black-box global optimization—Part I,” *IEEE Transactions on Evolutionary Computation*, vol. 26, no. 5, pp. 802–822, 2021.
- [29] —, “A review of population-based metaheuristics for large-scale black-box global optimization—Part II,” *IEEE Transactions on Evolutionary Computation*, vol. 26, no. 5, pp. 823–843, 2021.
- [30] X. Li, M. G. Eptropakis, K. Deb, and A. Engelbrecht, “Seeking multiple solutions: An updated survey on niching methods and their applications,” *IEEE Transactions on Evolutionary Computation*, vol. 21, no. 4, pp. 518–538, 2016.
- [31] N. Saini and S. Saha, “Multi-objective optimization techniques: a survey of the state-of-the-art and applications: Multi-objective optimization techniques,” *The European Physical Journal Special Topics*, vol. 230, no. 10, pp. 2319–2335, 2021.
- [32] T. Weise, “Global optimization algorithms-theory and application,” *Self-Published Thomas Weise*, vol. 361, 2009.
- [33] É. J. Gouvêa, R. G. Regis, A. C. Soterroni, M. C. Scarabello, and F. M. Ramos, “Global optimization using q-gradients,” *European Journal of Operational Research*, vol. 251, no. 3, pp. 727–738, 2016.
- [34] M. Jamil and X.-S. Yang, “A literature survey of benchmark functions for global optimisation problems,” *International Journal of Mathematical Modelling and Numerical Optimisation*, vol. 4, no. 2, pp. 150–194, 2013.
- [35] J. J. Moré, B. S. Garbow, and K. E. Hillstom, “Testing unconstrained optimization software,” *ACM Transactions on Mathematical Software (TOMS)*, vol. 7, no. 1, pp. 17–41, 1981.
- [36] M. Molga and C. Smutnicki, “Test functions for optimization needs,” *Test functions for optimization needs*, vol. 101, p. 48, 2005.
- [37] R. Chelouah and P. Siarry, “Genetic and nelder–mead algorithms hybridized for a more accurate global optimization of continuous multimimima functions,” *European Journal of operational research*, vol. 148, no. 2, pp. 335–348, 2003.
- [38] N. Awad, M. Ali, J. Liang, B. Qu, and P. Suganthan, “Problem definitions and evaluation criteria for the CEC 2017 special session and competition on single objective bound constrained real-parameter numerical optimization,” Tech. Rep., 2016.

- [39] C. Yue, K. V. Price, P. N. Suganthan, J. Liang, M. Z. Ali, B. Qu, N. H. Awad, and P. P. Biswas, "Problem definitions and evaluation criteria for the CEC 2020 special session and competition on single objective bound constrained numerical optimization," Tech. Rep., 2019.
- [40] D. Yazdani, *Generalized Numerical Benchmark Generator (GNBG)-Instance Generator (MATLAB Source Code)*, 2023 (accessed December 10, 2023). [Online]. Available: <https://github.com/Danial-Yazdani/GNMG-Generator>
- [41] M. N. Omidvar, M. Yang, Y. Mei, X. Li, and X. Yao, "DG2: A faster and more accurate differential grouping for large-scale black-box optimization," *IEEE Transactions on Evolutionary Computation*, vol. 21, no. 6, pp. 929–942, 2017.
- [42] D. Yazdani, M. N. Omidvar, D. Yazdani, J. Branke, T. T. Nguyen, A. H. Gandomi, Y. Jin, and X. Yao, "Robust optimization over time: A critical review," *IEEE Transactions on Evolutionary Computation*, 2023.
- [43] K. De Jong, "Evolving in a changing world," in *International Symposium on Methodologies for Intelligent Systems*. Springer, 1999, pp. 512–519.
- [44] D. Yazdani, "Particle swarm optimization for dynamically changing environments with particular focus on scalability and switching cost," Ph.D. dissertation, Liverpool John Moores University, Liverpool, UK, 2018.
- [45] V. Torczon, "On the convergence of pattern search algorithms," *SIAM Journal on optimization*, vol. 7, no. 1, pp. 1–25, 1997.
- [46] J. Kennedy and R. Eberhart, "Particle swarm optimization," in *Proceedings of ICNN'95-International Conference on Neural Networks*, vol. 4. IEEE, 1995, pp. 1942–1948.
- [47] M. R. Bonyadi and Z. Michalewicz, "Particle swarm optimization for single objective continuous space problems: a review," pp. 1–54, 2017.
- [48] R. Storn and K. Price, "Differential evolution—a simple and efficient heuristic for global optimization over continuous spaces," *Journal of global optimization*, vol. 11, pp. 341–359, 1997.
- [49] S. Das and P. N. Suganthan, "Differential evolution: A survey of the state-of-the-art," *IEEE transactions on Evolutionary Computation*, vol. 15, no. 1, pp. 4–31, 2010.
- [50] M. A. Abramson, C. Audet, J. E. Dennis Jr, and S. L. Digabel, "Orthomads: A deterministic mads instance with orthogonal directions," *SIAM Journal on Optimization*, vol. 20, no. 2, pp. 948–966, 2009.
- [51] C. Audet and J. E. Dennis Jr, "Analysis of generalized pattern searches," *SIAM Journal on optimization*, vol. 13, no. 3, pp. 889–903, 2002.
- [52] R. Eberhart and Y. Shi, "Comparing inertia weights and constriction factors in particle swarm optimization," in *IEEE Congress on Evolutionary Computation*, vol. 1. IEEE, 2001, pp. 84–88.